Atmos. Chem. Phys. Discuss., https://doi.org/10.5194/acp-2017-903
Manuscript under review for journal Atmos. Chem. Phys.
Discussion started: 14 November 2017


Atmospheric Chemistry and Physics Discussions

# Importance of reactive halogens in the tropical marine atmosphere: A regional modelling study using WRF-Chem

Alba Badia[1], Claire E. Reeves[1], Alex R. Baker[1], Alfonso Saiz-Lopez[2], Rainer Volkamer[3,4], Eric C. Apel[4], Rebecca S. Hornbrook[4], Lucy J. Carpenter[5], Stephen J. Andrews[5], and Roland von Glasow[1,*]

[1]Centre for Ocean and Atmospheric Sciences, School of Environmental Sciences, University of East Anglia, Norwich, United Kingdom
[2]Department of Atmospheric Chemistry and Climate, Institute of Physical Chemistry Rocasolano, CSIC, Madrid, Spain
[3]Department of Chemistry and Biochemistry, University of Colorado, Boulder, CO, USA
[4]Earth System Laboratory, Atmospheric Chemistry Division, National Center for Atmospheric Research, Boulder, CO, USA
[5]Wolfson Atmospheric Chemistry Laboratories (WACL), Department of Chemistry, University of York, York, United Kingdom
[*]deceased, 6th September 2015

*Correspondence to:* a.badia-moragas@uea.ac.uk

**Abstract.**

This study investigates the impact of halogens on atmospheric chemistry in the tropical troposphere and explores the sensitivity of this to uncertainties in the fluxes of halogens to the atmosphere and the chemical processing. To do this the regional chemistry transport model WRF-Chem has been extended, for the first time, to include halogen chemistry (bromine, chlorine and iodine chemistry), including heterogeneous recycling reactions involving sea-salt aerosol and other particles, reactions of Br with volatile organic compounds (VOCs), along with oceanic emissions of halocarbons, VOCs and inorganic iodine. The study focuses on the tropical East Pacific using field observations from the TORERO campaign (January-February 2012) to evaluate the model performance.

Including all the new processes, the model does a reasonable job reproducing the observed mixing ratios of BrO and IO, albeit with some discrepancies, some of which can be attributed to difficulties in the model's ability to reproduce the observed halocarbons. This is somewhat expected given the large uncertainties in the air-sea fluxes of the halocarbons in a region where there are few observations of seawater concentrations. We see a considerable impact on the $Br_y$ partitioning when heterogeneous chemistry is included, with a greater proportion of the $Br_y$ in active forms such as BrO, HOBr and dihalogens. Including debromination of sea-salt increases BrO slightly throughout the free troposphere, but in the tropical marine boundary layer, where the sea-salt particles are plentiful and relatively acidic, debromination leads to overestimation of the observed BrO. However, it should be noted that the modelled BrO was extremely sensitive to the inclusion of reactions between Br and the VOCs, which convert Br to HBr, a far less reactive form of $Br_y$. Excluding these reactions leads to modelled BrO mixing ratios greater than observed. The reactions between Br and aldehydes were found to be particularly important, despite the model underestimating the amount of aldehydes observed in the atmosphere. There are only small changes to $I_y$ partitioning and IO when the heterogeneous reactions, primarly on sea-salt, are included.

Atmos. Chem. Phys. Discuss., https://doi.org/10.5194/acp-2017-903
Manuscript under review for journal Atmos. Chem. Phys.
Discussion started: 14 November 2017


Atmospheric Chemistry and Physics Discussions

Our model results show that the tropospheric $O_x$ loss due to halogens is 31%. This loss is mostly due to I (16%) and Br (14%) and it is in good agreement with other estimates from state-of-the-art atmospheric chemistry models.

## 1 Introduction

Reactive halogens cause ozone ($O_3$) destruction, change the $HO_X$ ($HO_2$ + OH) and $NO_X$ ($NO_2$ + NO) partitioning, affect the oxidation of VOCs and mercury, reduce the lifetime of methane, and take part in new particle formation (Chameides and Davis, 1980; von Glasow et al., 2004; Saiz-Lopez and von Glasow, 2012). Halogen species are known to play an important role in the oxidising capacity of the troposphere. The atmospheric oxidation capacity is to a large extent determined by the hydroxyl radical (OH), $O_3$ and their budgets and cycling; globally most tropospheric OH is found in the tropics (Bloss et al., 2005). Therefore a quantitative understanding of the composition and chemistry of the tropical marine atmosphere is essential to examine the atmospheric oxidative capacity and climate forcing.

In the troposphere, reactive halogen species catalyse ozone destruction cycles:

$$O_3 + X \rightarrow XO + O_2 \quad \text{(R1)}$$

$$HO_2 + XO \rightarrow HOX + O_2 \quad \text{(R2)}$$

$$HOX + h\nu \rightarrow OH + X \quad \text{(R3)}$$

where X= Cl, Br, I.

Numerical models predict that reactive halogen compounds account for 30% of $O_3$ destruction in the MBL (von Glasow et al., 2002b, 2004; Saiz-Lopez et al., 2015; Sherwen et al., 2016b) and 5-20% globally (Yang et al., 2005; Saiz-Lopez et al., 2015, 2012a; Sherwen et al., 2016b). Up to 34% of $O_3$ loss is calculated to be due to I and Br combined in the tropical East Pacific (Wang et al., 2015). In the past, tropospheric halogen chemistry has been studied using a number of box models and 1D models (Sander and Crutzen, 1996; von Glasow et al., 2002a; Saiz-Lopez et al., 2006; Simpson et al., 2015; Lowe et al., 2009; Sommariva and von Glasow, 2012). Currently, there are several global models that have been used to study tropospheric halogens (Hossaini et al., 2010; Ordóñez et al., 2012; Saiz-Lopez et al., 2012a; Fernandez et al., 2014; Saiz-Lopez et al., 2015; Sherwen et al., 2016b; Schmidt et al., 2016). However, there are only a few regional models that have studied tropospheric halogens. Chlorine chemistry was implemented into the WRF-Chem model (Lowe et al., 2015; Li et al., 2016) and into the CMAQ model (Sarwar et al., 2014) to study the formation of nitryl chloride ($ClNO_2$) from the uptake of dinitrogen pentoxide ($N_2O_5$) on aerosols containing chloride. Moreover, bromine and iodine chemistry was implemented in CMAQ in Gantt et al. (2017) and Sarwar et al. (2015), where the impact of iodide-mediated $O_3$ deposition on surface ozone concentrations was studied, and in the recent work of Muñiz-Unamunzaga et al. (2017), that concluded that oceanic halogens and dimethyl sulfide (DMS) emissions need to be included into the regional models to accurately reproduce the air quality in coastal cities.

Oceanic emissions provide Very Short Lived Halocarbons (VSLH) to the atmosphere, mainly in the form of bromoform ($CHBr_3$), dibromomethane ($CH_2Br_2$) and methyl iodide ($CH_3I$). Once in the atmosphere, VSLH (and their degradation prod-

Atmos. Chem. Phys. Discuss., https://doi.org/10.5194/acp-2017-903
Manuscript under review for journal Atmos. Chem. Phys.
Discussion started: 14 November 2017


Atmospheric Chemistry and Physics Discussions

ucts) can ascend into the lower stratosphere (LS) where they can contribute to the inorganic bromine ($Br_y$) and lead to ozone depletion. Several emissions inventories for the VSLH have been evaluated at a global scale (Bell et al., 2002; Ziska et al., 2013; Ordóñez et al., 2012; Hossaini et al., 2013; Lennartz et al., 2015). Lennartz et al. (2015) presents a comparison of two simulations using the chemistry climate model EMAC. The first simulation computes the oceanic emissions online, mainly driven by the surface water concentrations and modelled meteorological variables, and the second uses prescribed emissions. These results reveal that calculating the air-sea fluxes online leads, in most cases, to more accurate atmospheric mixing ratios in the model in comparison with the simulation using prescribed emissions. Emissions of inorganic iodine compounds (HOI and $I_2$) have been recognised as a significant source required to reproduce iodine oxide (IO) measurements over the open ocean (Mahajan et al., 2012; Carpenter et al., 2013) and have been included in some global models (Saiz-Lopez et al., 2014; Sherwen et al., 2016b).

There are indications that the chemistry of reactive halogens and oxygenated VOCs (OVOCs) in the tropics are inter-related. Model calculations suggest aldehydes are an important sink for bromine atoms and hence compete with the formation of BrO ($Br + O_3 \rightarrow BrO$). This illustrates a link between the cycles of halogens and OVOCs in the marine atmosphere (Sommariva and von Glasow, 2012; Toyota et al., 2004).

Recent studies have highlighted the key role that heterogeneous chemistry plays in explaining observations of BrO and IO abundances in the tropical troposphere. Cycling of Br and I through HOBr, $BrNO_3$, HOI and $INO_3$ is very slow in the gas-phase, making it necessary to include heterogeneous reactions to reproduce observed BrO and IO abundances (von Glasow et al., 2004; Saiz-Lopez et al., 2015; Sherwen et al., 2016a). Another source for reactive inorganic bromine in the troposphere is the release of bromine radicals by oxidation of bromide in sea-salt, known as debromination. This source has been included in several atmospheric models (Yang et al., 2005; Parrella et al., 2012; Ordóñez et al., 2012; Schmidt et al., 2016; Long et al., 2014). However, this process is poorly understood and its inclusion into the models can cause inconsistent levels of bromine species (Schmidt et al., 2016).

Atmospheric models remain largely untested due to lack of field observations of halogen species. However, during the last few years there have been four campaigns that provided vertically resolved measurements of halogen radicals: the Tropical Ocean tRoposphere Exchange of Reactive halogen species and Oxygenated VOC (TORERO; Volkamer et al., 2015; Wang et al., 2015; Dix et al., 2016), the CONvective TRansport of Active Species in the Tropics (CONTRAST; Pan et al., 2017; Koenig et al., 2017), the Coordinated Airborne Studies in the Tropics (CAST; Harris et al., 2017) and Airborne Tropical TRopopause EXperiment (ATTREX; Jensen et al., 2017).

The main objective of this study is to investigate the atmospheric chemistry in the tropical East Pacific with a focus on reactive halogens using the Weather Research and Forecasting model coupled with Chemistry (WRF-Chem; Grell et al., 2005) and field data from the TORERO campaign (Volkamer et al., 2015; Wang et al., 2015). Our reaction mechanism in WRF-Chem is based on the MOZART-4 mechanism (Emmons et al., 2010; Knote et al., 2014) and has been extended to include halogen chemistry. Heterogeneous recycling reactions have been included into the model, along with oceanic emissions of relevant VOCs and halocarbons. The observational data is described in Sec. 2. Model developments are described in Sec. 3. The model

Atmos. Chem. Phys. Discuss., https://doi.org/10.5194/acp-2017-903
Manuscript under review for journal Atmos. Chem. Phys.
Discussion started: 14 November 2017




setup and the description of different sensitivity runs are in Sec. 4. The results of the model performance are discussed in Sec. 5. The last section summarizes the conclusions of this work.

## 2 Observational data

The TORERO campaign (Volkamer et al., 2015; Wang et al., 2015), from 15 January to 1 March 2012, was used to evaluate the model. Data on halocarbons are available from the TORERO ship cruise (Andrews et al., 2015) and flights, whilst observations of $O_3$, BrO, IO and oxygenated VOCs (OVOCs) are available from the flights. The TORERO cruise aboard the NOAA RV Ka'imimoana (KA-12-01) took place from Honolulu, HI, to Puntarenas, Costa Rica, between 27 January and 1 March 2012. BrO and IO were further measured aboard the NSF/NCAR GV aircraft with typical detection limits of 0.5 pptv for BrO, and 0.05 pptv for IO (Volkamer et al., 2015; Dix et al., 2016). 13 flights provide $O_3$ data and 16 flights provide BrO and IO data. Fig. 1 displays the location of all the observational data with an orange line for the cruise track, red lines for the flights in the tropics and green lines for the flights in the sub-tropics.

## 3 Model description

WRF-Chem (Grell et al., 2005) is a highly flexible community model for atmospheric research where aerosol-radiation-cloud feedback processes are taken into account. Version 3.7.1 is used in this study.

### 3.1 Oceanic fluxes

The oceanic emission of inorganic iodine (HOI and $I_2$) follows the deposition of $O_3$ to the surface ocean and reaction with iodide ($I^-$) (Carpenter et al., 2013). We use Eqs. 19 and 20 in Carpenter et al. (2013) for the calculation of these emissions. Ocean surface $I^-$ is parameterized using MacDonald et al. (2014) (see Fig. S1 in the supplementary information). Fig. 2 shows the average oceanic emission for inorganic iodine ($I_2$ in the left and HOI in the middle panels) during January and February 2012. Higher emissions for inorganic iodine occurs in the tropics with HOI being the dominant species.

Two different approaches for the marine emissions of the halocarbons ($CHBr_3$, $CH_2Br_2$, $CH_3I$, $CH_2BrCl$, $CHBrCl_2$, $CHBr_2Cl$, $CH_2I_2$, $CH_2IBr$ and $CH_2ICl$) are examined in this model. The first approach uses prescribed monthly average oceanic fluxes from Ziska et al. (2013) and the second computes the oceanic fluxes online. Computing the emissions online accounts for an interaction between the modelled atmosphere and the ocean at each time step. Thus, this approach can respond to changes in meteorological parameters, like surface temperature and surface wind speed. The two-layer model (Liss and Slater, 1974) is used to calculate the halocarbons air-sea fluxes:

$$F = -K_a \cdot (C_g - K_H \cdot C_l) \quad (1)$$

where $K_a$ is the transfer velocity of the gas ($s^{-1}$), $C_g$ (ppm) and $C_l$ (nM) are the bulk gas and liquid-phase concentrations and $K_H$ is the Henry's law constant. $K_a$ is parameterized following Johnson (2010) which is mainly a function of wind speed and

Atmos. Chem. Phys. Discuss., https://doi.org/10.5194/acp-2017-903
Manuscript under review for journal Atmos. Chem. Phys.
Discussion started: 14 November 2017


Atmospheric Chemistry and Physics Discussions

sea surface temperature (SST) taken from the model at each time-step. $C_g$ is also taken from the model. Halocarbon sea-water concentrations $C_l$ are taken from Ziska et al. (2013). Fig. 3 shows the average air-sea fluxes for $CHBr_3$, $CH_2Br_2$ and $CH_3I$ during January and February 2012 for the two approaches. Note that, the online calculation could increase, decrease or even reverse the fluxes in comparison with the prescribed emissions. This is the case for the online fluxes of $CHBr_3$ over the tropics where the model calculates negative fluxes whereas the prescribed fluxes are positive.

Recent studies suggest that the ocean is an important source of OVOCs (Coburn et al., 2014; Lawson et al., 2015; Mahajan et al., 2014; Myriokefalitakis et al., 2008; Sinreich et al., 2010; Volkamer et al., 2015) that the models do not consider or are not able to capture (Millet et al., 2010; Sherwen et al., 2016a). Thus, oceanic fluxes of several VOCs have been included into the model. The same online approach is done for three OVOCs (acetaldehyde ($CH_3CHO$), ethanol ($C_2H_6O$) and methanol ($CH_3OH$)) where their sea-water concentrations are taken from Yang et al. (2014). Emissions for alkenes and alkanes ($C_2H_4$, $C_3H_6$, $C_2H_6$, $C_3H_8$) are prescribed and based on the POET (Granier et al., 2005) global inventory.

Deposition over the ocean for the halocarbons and OVOCs is included in the air-sea fluxes described above. For the rest of the species, dry deposition is calculated with the Wesely scheme (Wesely, 1989), which is used over land for several species. Washout of gases by precipitation is simulated using the scheme included in WRF-Chem (Grell and Dévényi, 2002; Zaveri et al., 2008) which was modified to include the Henry's law constants for the halogens shown in Table 1.

The sea-salt aerosol emissions parameterization used in this study is described in Archer-Nicholls et al. (2014). This parameterization is mainly a function of wind speed from the model.

### 3.2 Gas-phase chemistry scheme

Our reaction mechanism is based on the MOZART-4 mechanism (Emmons et al., 2010; Knote et al., 2014). This mechanism has been extended to include bromine, chlorine and iodine chemistry and has been coupled with the MOSAIC 4-bin aerosol module (Zaveri et al., 2008). A total of 48 species and 159 halogen reactions have been included (see Tables 2, 3 and 4 for details). Most of these reactions come from the 1D model MISTRA (Sommariva and von Glasow, 2012) which includes inorganic, organic and inter-halogens reactions. Production and loss reactions of the higher order of iodine oxides ($I_2O_X$, where X=2,3,4) reactions have been included into the model. Photochemistry of $I_2O_X$ species is still an aera of high uncertainty in atmospheric iodine chemistry (Sommariva et al., 2012; Saiz-Lopez et al., 2012b). Chemical loss of VSLH through oxidation by the hydroxyl radical (OH) and by photolysis is included using data from Sander et al. (2011b).

A schematic representation of the main bromine and iodine chemistry implemented in the model is shown in Fig 4. Chlorine chemistry is also included into the model, however, since our results are mainly focused on reactive bromine and iodine, we do not include chlorine chemistry in Fig 4.

Photolysis reactions included in the mechanism are listed in Table 4. To compute the photolysis rates the Fast Tropospheric Ultraviolet-Visible (FTUV) online scheme (Tie et al., 2003) is used. The quantum yields and cross section for the photolytic reactions of halogens are from JPL 10-6 (Sander et al., 2011b) and have been linearly interpolated onto the 17 bins used by FTUV. For $I_2O_X$ we use the quantum yield and cross section data from Gómez Martín et al. (2005).

Atmos. Chem. Phys. Discuss., https://doi.org/10.5194/acp-2017-903
Manuscript under review for journal Atmos. Chem. Phys.
Discussion started: 14 November 2017


Atmospheric Chemistry and Physics Discussions

#### 3.2.1 Halogens and VOCs reactions

Reactions between halogens and VOCs can be important for regulating reactive halogen chemistry in the MBL by promoting the conversion of Cl and Br atoms into HCl and HBr or more stable organic halogenated intermediates. The oxidation of methane ($CH_4$), formaldehyde ($CH_2O$), acetaldehyde ($CH_3CHO$), methanol ($CH_3OH$), methyl hydroperoxide ($CH_3OOH$), methylperoxy ($CH_3O_2$), ethane ($C_2H_6$), ethene ($C_2H_4$) and propene ($C_3H_6$) by Cl is included in the chemical mechanism. In addition, the oxidation of $CH_2O$ and $CH_3CHO$ by bromine is also included in the chemical mechanism. A simplified version of the chemical scheme presented in Toyota et al. (2004) for reactions of bromine with alkenes is included:

$$\mathrm{Br} + \mathrm{C_2H_4} + \mathrm{O_2} \rightarrow \mathrm{BrRO_2} \quad \text{(R4)}$$

$$\mathrm{Br} + \mathrm{C_3H_6} + \mathrm{O_2} \rightarrow \mathrm{BrRO_2} \quad \text{(R5)}$$

where $BrRO_2$ is a brominated peroxy radical.

The decay of $BrRO_2$ is defined as:

$$\mathrm{BrRO_2} + \mathrm{NO} \rightarrow x\mathrm{HBr} + (1-x)\mathrm{Br} + \mathrm{CH_3CO_3} + \mathrm{NO_2} + 0.5\mathrm{CH_2O} + \mathrm{HO_2} \quad \text{(R6)}$$

$$\mathrm{BrRO_2} + \mathrm{CH_3O_2} \rightarrow x\mathrm{HBr} + (1-x)\mathrm{Br} + \mathrm{CH_3CO_3} + \mathrm{HO_2} + \mathrm{CH_2O} \quad \text{(R7)}$$

$$\mathrm{BrRO_2} + \mathrm{HO_2} \rightarrow \mathrm{BrOR} + \mathrm{H_2O} \quad \text{(R8)}$$

The decay of BrOR is defined as:

$$\mathrm{BrOR} + \mathrm{OH} \rightarrow 0.5(x\mathrm{HBr} + (1-x)\mathrm{Br}) + 0.5\mathrm{BrRO2} + 0.5\mathrm{OH} + 0.5\mathrm{CH_3CHO} \quad \text{(R9)}$$

$$\mathrm{BrOR} + h\nu \rightarrow x\mathrm{HBr} + (1-x)\mathrm{BrOH} + \mathrm{HO_2} + \mathrm{CH_3CO_3} + 0.5\mathrm{CH_2O} \quad \text{(R10)}$$

where BrOR is a brominated organic specie and $x$ is a number between 0 and 1.

Reaction rates for these reactions and deposition velocities are taken from Toyota et al. (2004). Kinetic data for these reactions is poor, and the partitioning of the products (HBr/Br) is not clear. Based on the Toyota et al. (2004) description, it is assumed that $x = 0.2$ such that the partitioning for HBr/Br is 1/4 (Toyota, pers. comm., 2017).

### 3.3 Heterogeneous chemistry

Heterogeneous reactions on particle surfaces involving halogens are summarised in Table 5. The heterogeneous chemistry is assumed to take place between a gas-phase species and an adsorbed species. Uptake coefficients are used to calculate first-order rate constants for heterogeneous loss of the gas-phase to the adsorbing surface (Jacob, 2000). Thus, the reaction rate constants, K ($s^{-1}$), are given by:

$$K = \frac{\gamma}{4} \cdot S \cdot A \quad (2)$$

Atmos. Chem. Phys. Discuss., https://doi.org/10.5194/acp-2017-903
Manuscript under review for journal Atmos. Chem. Phys.
Discussion started: 14 November 2017


Atmospheric Chemistry and Physics Discussions

where $\gamma$ is the uptake coefficient, S is the root-mean-square molecular speed (m $s^{-1}$) and A is the total available aerosol surface area density ($cm^2$ $cm^{-3}$). Second-order reaction rate constants are calculated by dividing the first-order rate constant by the concentrations of the adsorbed species. Heterogeneous halogen activation is very efficient under cold or stratospheric conditions as compared to moderate temperatures. For this reason, we have made a distinction between moderate (> 243.15 K) and cold temperatures (< 243.15 K) in some reactions. Uptake coefficients for reactions in Table 5 are based on literature values where available (Jacob, 2000; Sander et al., 2006; Ordóñez et al., 2012).

Bulk aqueous phase chemistry in sea-salt aerosols is not treated in this study. Instead, we use a free molecular transfer regime approximation following McFiggans et al. (2000), where the reaction rate is the first-order rate constant computed as described above. There are 6 reactions implemented for sea-salt particles. The sea-salt surface area is calculated in the following way: 1) using the mass of Na and Cl and the associated $H_2O$ for each bin and the individual dry densities (for Na, Cl and $H_2O$) the total volume of those particles for each bin is calculated and then, 2) assuming that sea-salt aerosols are spheres, the total surface area is calculated for each bin using this volume and the radius of aerosols in each bin.

It is known that the chemistry involving the release of bromine from the sea-salt aerosol is strongly pH dependent, being more efficient for acidified aerosol especially with a pH < 5.5 (Keene et al., 1998). For this reason, we apply a pH dependence for debromination reactions in sea-salt considering two cases: when the pH > 5.5 and when the pH < 5.5. The pH value of the aerosol particles is calculated in the model for each size bin (see Zaveri et al. (2008) for further description of the pH calculation). Thus, the following debromination reactions in sea-salt are only considered if the pH < 5.5:

$$\mathrm{BrNO_3} \rightarrow 0.6\mathrm{Br_2} + \mathrm{HNO_3} \quad \text{(R11)}$$

$$\mathrm{BrNO_2} \rightarrow 0.6\mathrm{Br_2} + \mathrm{HNO_3} \quad \text{(R12)}$$

$$\mathrm{HOBr} \rightarrow 0.6\mathrm{Br_2} \quad \text{(R13)}$$

$$\mathrm{INO_3} \rightarrow 0.5\mathrm{IBr} + 0.5\mathrm{ICl} + \mathrm{HNO_3} \quad \text{(R14)}$$

$$\mathrm{INO_2} \rightarrow 0.5\mathrm{IBr} + 0.5\mathrm{ICl} + \mathrm{HNO_3} \quad \text{(R15)}$$

$$\mathrm{HOI} \rightarrow 0.5\mathrm{IBr} + 0.5\mathrm{ICl} \quad \text{(R16)}$$

When the pH > 5.5 the following reactions are considered:

$$\mathrm{INO_3} \rightarrow 0.5\mathrm{I_2} + \mathrm{HNO_3} \quad \text{(R17)}$$

$$\mathrm{INO_2} \rightarrow 0.5\mathrm{I_2} + \mathrm{HNO_3} \quad \text{(R18)}$$

$$\mathrm{HOI} \rightarrow 0.5\mathrm{I_2} \quad \text{(R19)}$$

These reactions change the iodine speciation and add a net source for bromine if the marine aerosol is acidic.

Atmos. Chem. Phys. Discuss., https://doi.org/10.5194/acp-2017-903
Manuscript under review for journal Atmos. Chem. Phys.
Discussion started: 14 November 2017


Atmospheric Chemistry and Physics Discussions

Due to the high uncertainty in the debromination process, the fraction of $Br_2$ formed on reactions R11-R13 was chosen arbitrarily in order to add an extra bromine source in a simple way. A value of 0.6 was chosen. Fig. 2 shows the column-integrated fluxes for inorganic bromine ($Br_2$, right panel) during January and February 2012.

In addition, the heterogeneous uptake of $N_2O_5$ onto aerosol particles that contain $Cl^-$ to form $ClNO_2$ is considered in the model (see Lowe et al. (2015) for further description).

## 4 Model setup

The model is set up with a horizontal grid spacing of 30 km x 30 km and 30 vertical layers up to 50 hPa. Simulations that study the oxidation of VOCs by Br over the tropical area (described in Sec. 4.1) are performed with more vertical layers than the standard case in order to capture the vertical mixing in this area. Thus, 52 vertical layers up to 50h Pa are used in this case. The meteorological initial and lateral boundary conditions were determined using the ERA-Interim (Dee et al., 2011) data and the meteorology was reinitialized every 3 days to reproduce the observed transport. Chemical initial and boundary conditions (IC/BCs) are from the global atmospheric model GEOS-Chem described in Sherwen et al. (2016b). We conducted WRF-Chem simulations for January and February 2012 covering the TORERO domain (see Fig. 1). We performed a spin-up of 20 days. Table 6 describes the main configuration of the model.

### 4.1 Sensitivity studies

Eight different simulations were performed in this study. Our base simulation, WRF-DEBROM, considered all main processes involving halogen chemistry (sea-salt debromination, heterogeneous chemistry and reactions between halogens and VOCs) and computes the oceanic halocarbons fluxes online. The WRF-ZIS simulation is the same as WRF-DEBROM but uses prescribed oceanic emissions for the halocarbons. To account for the importance of the debromination in sea-salt particles, we run WRF-NODEBROM which is the same as WRF-DEBROM simulation but without debromination. WRF-NOHET simulation is the same as WRF-NODEBROM but without heterogeneous chemistry. A simulation with no halogen chemistry, WRF-NOHAL, is performed to study the effect of halogens on the tropospheric chemistry. All simulations except WRF-NOHAL use IC/BCs from the GEOS-Chem model that include halogens. WRF-NOHAL simulation uses IC/BCs from the GEOS-Chem model with no halogen chemistry. Finally, to study the oxidation of VOCs by Br three simulations have been performed: 1) a simulation without the reactions of bromine reactions with alkenes (WRF-NOALKE), 2) a simulation without the reactions of bromine with aldehydes (WRF-NOALD) and finally a simulation without the reactions of bromine with VOCs, therefore neither alkenes nor aldehydes (WRF-NOVOCS). See Table 7 for a summary of all these simulations.

Atmos. Chem. Phys. Discuss., https://doi.org/10.5194/acp-2017-903
Manuscript under review for journal Atmos. Chem. Phys.
Discussion started: 14 November 2017


Atmospheric Chemistry and Physics Discussions

## 5 Model results

This section presents the model evaluation with observations of relevant trace gases. The model output is sampled at the nearest timestamp and grid box to the measurements. An ocean mask neglecting grid-boxes above land was applied to compute all model results.

### 5.1 Oceanic emissions: Halocarbons

Fig. 5 shows the time series of $CHBr_3$ (top-left panel), $CH_2Br_2$ (top-right panel) and $CH_3I$ (bottom-left panel) mixing ratios (in ppt) for the WRF-ZIS (green line) and WRF-DEBROM (black line) runs. In addition, the modelled wind speed (black line) is also shown in Fig. 5 (bottom-right panel). Measurements for the halocarbons and wind speed are represented by the solid red lines. Fig. 6 presents the time series of $CHBr_3$, $CH_2Br_2$ and $CH_3I$ water concentration (in pmol/L) from the measurements (dashed red lines) and from the Ziska et al. (2013) climatology (dashed blue lines) used to compute both the prescribed and online fluxes.

In general, both simulations reproduce the concentrations of the halocarbons to the right order of magnitude, although there are specific periods with a negative bias. We see a tendency to underestimate $CHBr_3$ for both model simulations during most of the period. This result is similar to the study of Hossaini et al. (2016) who compared eleven global models using different emissions inventories. The majority of the models do not reproduce the observed concentrations in the tropical marine boundary layer. Over the tropics, high emissions observed are associated with tropical upwelling and active planktonic production (Class and Ballschmiter, 1988; Atlas et al., 1993). One reason for low $CHBr_3$ concentrations in our model simulations might be that the sea-water concentrations are too low in this area (see Fig. 6 for $CHBr_3$) and then the fluxes are also low (see Fig. S2 in the supplementary information). Note that Ziska et al. (2013) used only a very limited amount of data to compute the sea-water concentration for the halocarbons in a our domain, giving uncertainty in this input data when the fluxes are calculated. $CH_2Br_2$ is in good agreement with the observations despite a negative bias ($\sim$ -0.5ppt) between days 6-10 and 22-25 of February for both simulations. Bromocarbon concentrations in WRF-DEBROM agree better with the measurements, where the bias is decreased for specific periods (e.g. 20th February for $CHBr_3$ and 10th and 22nd February for $CH_2Br_2$) in comparison with WRF-ZIS. Moreover, the differences in correlation coefficients between simulations are: 0.48 and 0.3 for $CH_2Br_2$ and $CHBr_3$ in the case of WRF-ZIS and 0.65 and 0.43 for $CH_2Br_2$ and $CHBr_3$ in the case of WRF-DEBROM. Modelled $CH_3I$ concentrations show a similar trend to the observations, although, like the bromocarbons, both simulations present a negative bias during specific periods (days 6-10 and 18-28 of February). This underestimation is more prominent in the WRF-DEBROM simulation. One reason for that could be that the wind speed from WRF-Chem is lower than the wind speed used to calculate the prescribed emissions, producing lower online fluxes. The correlation coefficients changes for $CH_3I$, where 0.19 is calculated for the WRF-ZIS and 0.40 for the WRF-DEBROM simulation.

Specific periods of negative bias for both simulations demand further attention. A possible explanation for the underestimation in halocarbon atmospheric concentrations might be due to the input data (e.g. wind speed, SST, sea-water concentration) that we used to compute these fluxes. In the case of the online fluxes, between days 6-8 of February the model underestimates



wind speed and this is directly accompanied by an underestimation for all three halocarbons atmospheric concentrations. Ziska et al. (2013) demonstrate that changes in the input parameters, especially wind speed and SST, affect the fluxes calculation. The same study suggests that $CH_3I$ emissions are mainly influenced by variations of the wind speed. Moreover, the study of Lennartz et al. (2015), that uses the same sea-water concentration as our study, suggests that the negative bias in the modelled atmospheric concentrations could indicate regions where the sea-water concentration from the climatologies lacks hotspots, thus, missing an oceanic source regions. This is clearly seen for the sea-water concentrations of $CHBr_3$ (during most of the period), $CH_2Br_2$ (peaks around 15th February) and $CH_3I$ (peaks around 20th February) used in this study that seem to be too low in comparison with the observations (see Fig. 6). More data on the sea-water concentrations of these halocarbons in this region are required to better constrain the oceanic flux data sets available to models and so to improve the representation of these gases in the atmosphere.

### 5.2 Gas phase and heterogeneous chemistry: bromine and iodine partitioning

Fig. 7 compares model results sampled along 16 flight tracks with the observations for BrO (ppt) separating tropical from subtropical flights for the three simulations WRF-NOHET, WRF-NODEBROM and WRF-DEBROM. Results indicate that there is an improvement of the modelled BrO throughout the troposphere in both the tropics and subtropics when the heterogeneous chemistry is included in both tropics and subtropics.

In the subtropics, higher values of BrO are found in altitudes ranges 11-13 km due to the lower altitude of the tropopause. Some data points in this altitude range will be in the lower stratosphere. There is really good agreement with the observations particularly in the middle and upper troposphere where the model is able to capture the higher values of BrO. Within the model, aerosols over the subtropical area tend to be alkaline, thus, BrO does not increase in this area when sea-salt debromination is included. Over the tropics, where the aerosol is more acidic, elevated BrO is seen with the inclusion of the debromination (WRF-DEBROM) in the MBL where the sea-salt aerosols are mostly located (see emissions of $Br_2$ in Fig. 2). Debromination improves the simulation of BrO concentrations in the middle troposphere although it excessively increases BrO levels up to 1 ppt in the MBL. This overestimation is also seen in other modelling studies that include this process (Schmidt et al., 2016). Significant uncertainties still exist in sea-salt debromination processes and the parameterisations used here might be too simple to represent them.

In addition, the conversion of BrO to HBr is dominated by the reaction between Br and VOCs, such that the BrO overestimation seen in the MBL could be reduced if the modelled aldehydes concentrations increase (discussed in section 5.3). However, a reduction in the debromination would also reduce BrO concentrations. Thus, in order to capture the BrO concentrations in the MBL the right balance between these two chemical processes is needed. BrO is underestimated in the model by 1 ppt in the upper troposphere over the tropics. The breakdown of bromocarbons, such as $CHBr_3$, contributes to BrO concentrations in the UT, thus, a good representation of bromocarbons is needed. $CHBr_3$ is underestimated in the middle and upper troposphere especially over the tropics (see Fig. S3 in the supplementary information). The reason for that could be a combination of different factors: underestimation of the boundary conditions used in this study for $CHBr_3$, underestimation in the oceanic fluxes (see Fig. S2 in the supplementary information) and overestimation of the loss rates. Moreover, an underestimation in the

Atmos. Chem. Phys. Discuss., https://doi.org/10.5194/acp-2017-903
Manuscript under review for journal Atmos. Chem. Phys.
Discussion started: 14 November 2017


Atmospheric Chemistry and Physics Discussions

heterogeneous chemistry or uncertainties in the reactions between the halogens and VOCs (discussed in section 5.3) can also contribute to the underestimation of BrO in the UT over the tropics.

Fig. 8 shows the vertical profile distribution for inorganic bromine ($Br_y$ in ppt) for the three simulations WRF-NOHET (left panels), WRF-NODEBROM (middle panels) and WRF-DEBROM (right panels) over the subtropics (top panels) and tropics (bottom panels). Inorganic bromine concentrations increase with altitude with a maximum of 8 ppt at 14 km in the subtropical area for all three simulations. This reflects the lifetime of the bromocarbon species that breakdown and release Br in the UT and LS. Over the tropical area, inorganic bromine concentrations have a peak in the middle troposphere at 6 km and then decrease until 12 km then start to increase again. A big impact on the vertical $Br_y$ partitioning is seen between the three simulations. With the inclusion of the heterogeneous chemistry, there is a decrease of HBr and an increase of more reactive species: di-halogens (BrCl, $Br_2$ and BrI) and BrO. HOBr increases and $BrNO_3$ decreases in the UT due to $BrNO_3$ hydrolysis. Over the tropics, $Br_y$ increases in the MBL ($\sim$ 4ppt) when debromination is included (WRF-DEBROM). This enhancement is seen for all inorganic species with a maximum in the surface where the concentration of sea-salt aerosols is higher. Over the subtropical area, little differences are seen between WRF-NODEBROM and WRF-DEBROM.

Fig. 9 compares model results sampled along 16 flight tracks with the observations for IO separating tropical from sub-tropical flights for the three simulations WRF-NOHET, WRF-NODEBROM and WRF-DEBROM. No clear impact is seen with the inclusion of the heterogeneous chemistry. At the surface, simulations with heterogeneous chemistry (WRF-DEBROM and WRF-NODEBROM) have slightly lower IO concentrations than the simulation without heterogeneous chemistry (WRF-NOHET). The main reason for that reduction is the sink for the iodine oxides ($I_xO_y$) included in the heterogeneous chemistry. Over the tropical region, the model overestimated surface IO. This overestimation might be explained by the higher inorganic iodine oceanic fluxes in this area. Over the subtropics, IO enhancements observed below 4 km are not captured by the model. Some studies suggest that there is abiotic $CH_3I$ production when dust contacts seawater containing iodide (Williams et al., 2007). Implementing this chemistry into the model is out of the scope of this paper and further investigation is needed to explain whether the production of $CH_3I$ enhances the IO concentration or if there are other missing IO precursors. Gómez Martín et al. (2013) presented an analysis of observations of several gas-phase iodine species observations made during a field campaign in the eastern Pacific marine boundary layer and suggested that the presence of elevated $CH_3I$ does not have a big impact on the $IO_x$ concentrations due to $CH_3I$ in the MBL having a long lifetime ($\sim$2 days at the equator). An overestimation of modelled IO in the UT needs further investigation. This overestimation is similar to other modelling studies Sherwen et al. (2016a).

Fig. 10 shows the vertical profile distribution for inorganic iodine ($I_y$) for the three simulations WRF-NOHET (left panels), WRF-NODEBROM (middle panels) and WRF-DEBROM (right panels) over the subtropics (top panels) and tropics (bottom panels). $I_y$ is higher in the MBL where it is emitted, especially in the tropical region, with HOI being the dominant species. Concentrations start to decrease above the MBL due to the removal of soluble species by the wet deposition. Unlike $Br_y$, we do not see a big impact on the vertical partitioning distribution of $I_y$ with the inclusion of the heterogeneous chemistry. The only differences are the $I_y$ decreases in the surface with the inclusion of the heterogeneous chemistry, due to the removal of the iodine oxides, and the production of more di-halogens in the MBL, specially when debromination is included.

Atmos. Chem. Phys. Discuss., https://doi.org/10.5194/acp-2017-903
Manuscript under review for journal Atmos. Chem. Phys.
Discussion started: 14 November 2017


Atmospheric Chemistry and Physics Discussions

### 5.3 Impact on VOCs

Several VOCs oceanic fluxes have been included in the model (see section 3.2.1) as well as the oxidation of VOCs by halogens. In order to see the impact of halogen reactions with the VOCs, average loss rates of all organic compounds due to the Cl and Br families are calculated as % of the total tropospheric losses over the ocean for the WRF-DEBROM simulation. Bromine accounts for 9.2% of the oxidation of $CH_3CHO$, 1.4% of $CH_2O$, 0.8% of $C_2H_4$ and 4.1% of $C_3H_6$. Chlorine accounts for 0.6% of the oxidation of $CH_3CHO$, 0.3% of $CH_2O$, 7.7% of $CH_3OH$, 0.8% of $CH_3OOH$, 0.6% of $CH_3O_2$, 35.5% of $C_2H_6$ and 10.5% of $C_3H_8$.

A sub-set of 9 flights from the TORERO campaign over the tropics is compared with the WRF-DEBROM, WRF-NOVOCS, WRF-NOALKE and WRF-NOALD simulations for BrO (ppt) in Fig. 11. Comparisons between WRF-DEBROM and WRF-NOVOCS simulations show a clear difference (1-4 ppt) throughout the whole troposphere. VOCs play an important role in the MBL regulating the reactive halogens. Without the bromine reactions with the VOCs, the model clearly overestimates BrO in the MBL. In the middle and upper troposphere, where VOCs emitted from the ocean and large forests are transported by convection, the model underestimates the levels of BrO when these reactions have been considered. The results obtained indicate that the conversion of reactive into more stable species by these reactions might be too effective in these upper layers of the model.

In order to understand which families of VOCs have a higher impact on the BrO concentrations, the oxidation of alkenes and aldehydes by Br have been studied separately in WRF-NOALKE and WRF-NOALD simulations. Differences between WRF-DEBROM and WRF-NOALD are seen in the whole troposphere with higher differences in the MBL up to 2ppt, where the concentrations of both bromine and aldehydes are high. Aldehydes concentrations are underestimated by the model, especially for $CH_3CHO$, meaning that BrO modelled concentrations would be even lower if the modelled aldehydes concentrations were reconciled with the observations. Small differences are observed between WRF-DEBROM and WRF-NOALKE. However, differences up to 2 ppt between WRF-NOVOCS and WRF-NOALD are clearly seen especially in the MBL.

These findings suggest that when aldehyde oxidation by Br is included, $Br_Y$ is reduced considerable, thus, limiting the amount of alkenes oxidation by Br (difference between WRF-DEBROM and WRF-NOALKE). However, when the oxidation of aldehydes is included, there is sufficient $Br_Y$ present for the oxidation of alkenes by Br to have an impact on the BrO (difference between WRF-NOALD and WRF-NOVOCS).

From this, we concluded that VOCs have an important role in the reactive bromine concentrations and VOCs marine emissions as well as halogen reactions with VOCs need to be included into the models. However, uncertainty still exists in some of these reactions (see Sec. 3.2.1).

### 5.4 Impact on $O_3$ and $O_x$

Fig. 12 (left panel) presents a comparison of 2 model simulations (WRF-DEBROM, WRF-NOHAL) sampled along 13 flight tracks with the observations for $O_3$ (ppb). The model is in line with the observations, capturing the $O_3$ gradient and variability of data throughout the troposphere. The average difference between the two simulations throughout the troposphere is 6.7 ppb.

Atmos. Chem. Phys. Discuss., https://doi.org/10.5194/acp-2017-903
Manuscript under review for journal Atmos. Chem. Phys.
Discussion started: 14 November 2017




In the MBL, high concentrations of halogens due to ocean emissions destroy $O_3$ and contribute to a negative bias up to 8 ppb. In the middle troposphere, the model results improve with the inclusion of halogens, where the average bias is reduced from 4. to -2.4 ppb. In the upper troposphere, where the differences between the two simulations are mainly driven by the boundary conditions used for each simulation, both simulations underestimate the ozone concentrations.

Fig. 12 (middle and right panels) shows the regional effects of halogen chemistry on simulated $O_3$ concentrations at the surface. Surface mean bias (ppb) and relative mean bias (%) between the simulation with no halogen chemistry (WRF-NOHAL) and with halogen chemistry (WRF-DEBROM) for the simulation period are presented. We find that the regional $O_3$ concentrations are reduced between 2-18 ppb, corresponding to 25-70 %, with the inclusion of the halogens. Over the tropics, there is a substantial decrease of $O_3$ (> 8ppb, > 40%). As we see in Fig. 2 and 3, there are high iodine and bromocarbon emissions and especially high bromine produced from debromination over this area. These destroy ozone and contribute to higher difference in $O_3$ concentrations in this area.

The odd oxygen $O_x$ is defined as:

$O_x = O(^3P) + O(^2D) + O_3 + NO_2 + 2\times NO_3 + HNO_3 + HO_2NO_2 + 3\times N_2O_5 + PAN + MPAN + ONIT + ONITR + ISOPNO_3 + PBZNIT + MBONO_3O_2 + XO + HOX + XNO_2 + 2\times XNO_3 + 2\times OIO + 2\times I_2O_2 + 3\times I_2O_3 + 4\times I_2O_4 + 2\times OClO$,

where X=Cl, Br and I; PAN= peroxyacetyl nitrate, MPAN= methacryloyl peroxynitrate; ONIT= organic nitrate; ONITR= lumped isoprene nitrate; $ISOPNO_3$= peroxy radical from $NO_3$+ISOP; PBZNIT= peroxybenzoyl nitrate; $MBONO_3O_2$= peroxy radical from $NO_3$ + 2 methyl-3-buten-2-ol.

The $O_x$ loss is divided by ozone depleting families ($O_x$ , $HO_x$, $NO_y$, VOCs, Br, Cl and I). Note that to calculate the $O_x$ loss due to the $O_x$ depleting family we only consider reactions involving $O(^3P)$, $O(^2D)$ and $O_3$. The average tropospheric vertical $O_x$ loss grouped by ozone depleting families for the WRF-DEBROM simulation is given in Fig. 13. Table 8 summarises the relative contribution of each family averaged at different altitude intervals.

The regional average $O_x$ percentage loss due to the halogens in our model domain is 34%, 18% and 40% in the MBL (p>900hPa), FT (350<p<900hPa) and UT (350hPa<p<trop), respectively. The MBL $O_x$ loss is in good agreement with Sherwen et al. (2016b) that reported 33% and Prados-Roman et al. (2015) reported 31%. The tropospheric $O_x$ loss due to the bromine, iodine and chlorine is 14%, 16%, 1%, respectively. The very fast catalytic reactions of iodine species make the iodine loss higher than for bromine and chlorine, especially in the MBL (19%). With the inclusion of the sea-salt debromination, $O_x$ loss due to the bromine is 14% in the MBL. In the upper troposphere, iodine contributes 21% and bromine 19% to the total $O_x$ loss. Thus, the overall impact of halogen chemistry on the tropospheric $O_x$ loss is 31 %. This value is comparable with other studies that reported 28% over the tropics (Saiz-Lopez et al., 2015) and 21.4% at the global scale (Sherwen et al., 2016b). Moreover, our results are in agreement with Wang et al. (2015), that used a box model and concluded that bromine and iodine are responsible for 34% of the column-integrated loss of tropospheric $O_3$. The tropospheric $O_x$ loss due to the iodine is higher than the box model study of Dix et al. (2013), that concluded that the fraction of iodine-induced ozone loss generally is around 10%.

Atmos. Chem. Phys. Discuss., https://doi.org/10.5194/acp-2017-903
Manuscript under review for journal Atmos. Chem. Phys.
Discussion started: 14 November 2017




## 6 Conclusions

We have presented a regional 3D tropospheric model that includes halogen chemistry (bromine, iodine and chlorine). A comprehensive description has been provided for the halogen gas-phase chemistry, the heterogeneous recycling reactions in sea-salt aerosol and other particles, reactions of Br with volatile organic compounds (VOCs) and the oceanic emissions of halocarbons, inorganic iodine and several VOCs. It is the first time that a halogen chemistry mechanism has been implemented into the online WRF-Chem model. Our results provide useful insight regarding the potential importance of reactive halogens in the tropical marine atmosphere. Field data from the TORERO campaign (Jan-Feb 2012) has been used in the model evaluation.

Two different approaches to compute marine emissions, online and prescribed, for the very short-lived halocarbons are discussed here. There is an improvement using online fluxes, WRF-DEBROM, in comparison with prescribed fluxes, WRF-ZIS, especially for $CH_2Br_2$ and $CHBr_3$, where the bias is decreased for specific periods. During the whole period, an underestimation is seen for both simulations for $CHBr_3$. This underestimation is similar to other modelling studies, which indicates the oceanic fluxes for $CHBr_3$ in this region are not well determined. Results indicate that the input data (especially wind-speed and water concentrations) used in this study to calculate marine fluxes underestimate halocarbon concentrations.

Three sensitivity studies are compared in order to understand the impact of the heterogeneous chemistry for bromine and iodine species. Results show that the inclusion of heterogeneous chemistry on marine aerosol has a considerable impact on the $Br_y$ partitioning, increasing reactive species like BrO. An increase of $Br_y$ is seen in the tropical MBL when debromination processes are included, due to the presence of relatively acidic particles. The oxidation of alkenes and aldehydes by bromine have been studies in three different sensitivity runs. These runs suggest that reactions of bromine with VOCs have a big impact on the BrO concentrations. The reactions between Br and aldehydes were found to be particularly important, despite the model underestimating the amount of aldehydes observed in the atmosphere.

The model shows an overall good agreement for the IO vertical profile. Higher modelled concentrations in the surface are seen over the tropics indicating that inorganic iodine emissions might be too high in this area. The model is not able to capture the IO enhancements sometimes seen below 4 km over the subtropical area. Unlike, $Br_y$, the $I_y$ partitioning is found to be relatively insensitive to inclusion of the heterogeneous chemistry.

Halogens constitute 31% of the overall tropospheric $O_x$ loss. This value is comparable with other studies. The tropospheric $O_x$ loss due to the bromine, iodine, and chlorine is 14%, 16%, 1%, respectively. The model captures the $O_3$ vertical profile in the free troposphere. However, a negative bias (< 8 ppb) is seen in the MBL, where the oceanic emissions of the halogenated species are higher. Over the tropics, the regional surface $O_3$ concentrations are reduced between 2-18 ppb with the inclusion of the halogens.

Large uncertainties in the halogen chemistry still exists: uptake coefficients in the heterogeneous chemistry, debromination process definition, photolytic rates (especially for the higher order of iodine oxides), wet scavenging and dry deposition of halogenated species, the chemical mechanism for the repartitioning of $Br_y$ resulting from the reactions of Br with VOCs, inputs to calculate the oceanic fluxes (e.g. sea-water concentration), etc. Some of these processes counteract each other, e.g. inclusion of debromination increases BrO, whilst reactions between Br and VOCs decrease BrO, making it difficult to assess



through evaluation against observations of a limited number of chemical species if any one process improves the modelled representation of the chemistry, or not. More data is required at the process level from laboratory studies along with field observations of, for example, more $Br_y$ and $I_y$ species, to better constrain the modelled representation of these processes and to verify if halogens really do have such a large impact on $O_x$ in the tropical troposphere. This is important given that the oxidising capacity of this region of the atmosphere has a large impact on the lifetime of many pollutants including methane, a key greenhouse gas.

*Acknowledgements.* This work is funded by a National Environmental Research Council (NERC) grant. The authors wish to thank the TORERO team, specially Barbara Dix and Theodore Konstantinos. TORERO was supported by NSF under award AGS-1104104 (PI: R.Volkamer). The involvement of the NSF-sponsored Lower Atmospheric Observing Facilities, managed and operated by the National Center for Atmospheric Research (NCAR) Earth Observing Laboratory (EOL), is acknowledged. R.V. acknowledges funding from NSF award AGS-1620530. L.J.C. acknowledges support from NERC (award NE/J00619X/1). Also, thanks to Mat Evans and Tomás Sherwen for providing the GEOS-Chem data and Carlos Cuevas, Douglas Lowe, Gordon McFiggans, Kenjiro Toyota, Peter Braüer and Roberto Sommariva for their constructive suggestions and feedback during this study. Finally, this work is specially dedicated to the friendship and memory of Professor Roland von Glasow.

Atmos. Chem. Phys. Discuss., https://doi.org/10.5194/acp-2017-903
Manuscript under review for journal Atmos. Chem. Phys.
Discussion started: 14 November 2017


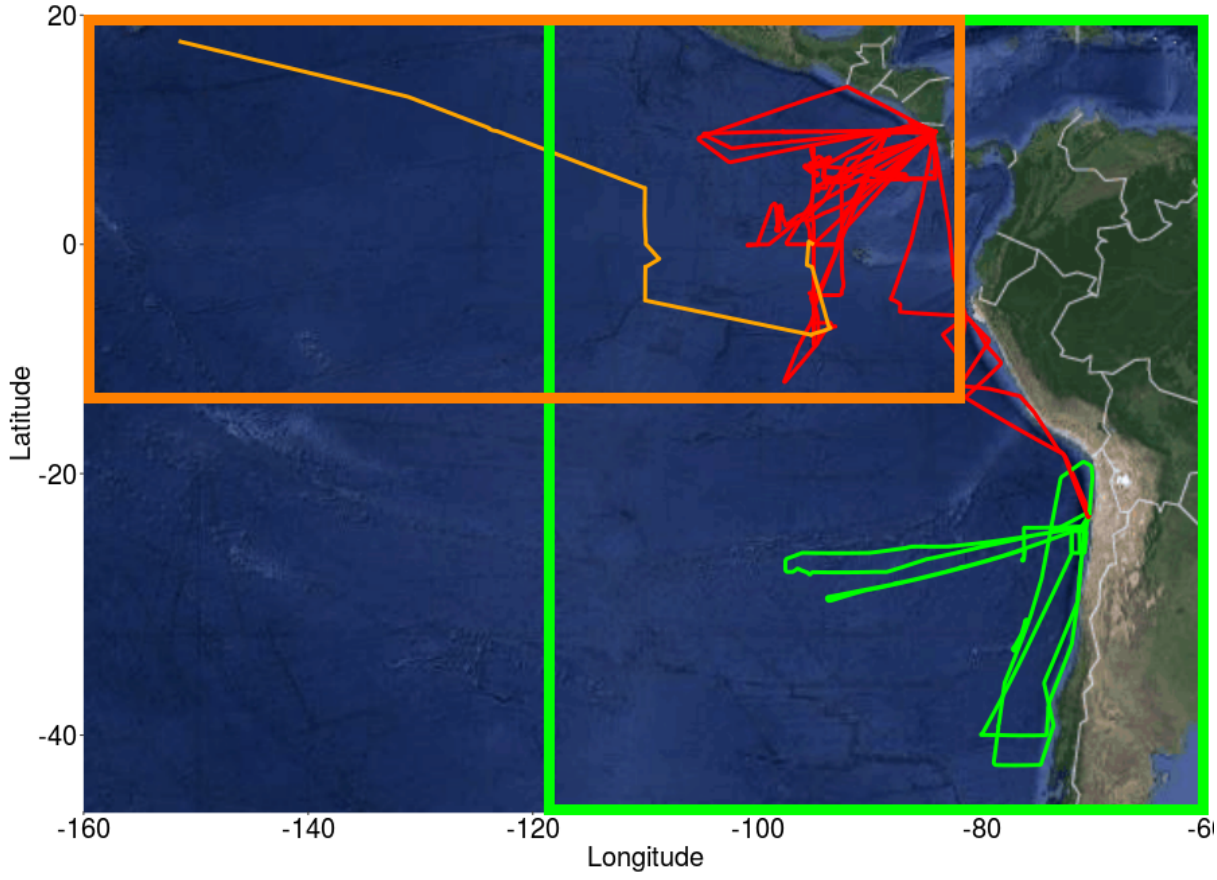


**Figure 1.** Flight and cruise tracks from the TORERO campaign (January-February 2012). Cruise track is represented by an light orange line. Flights are grouped by the following regions: tropical (red lines) and subtropical (green lines). Two different domains where defined: domain to evaluate the cruises (dark orange square) and domain to evaluate aircrafts (green square).

Atmos. Chem. Phys. Discuss., https://doi.org/10.5194/acp-2017-903
Manuscript under review for journal Atmos. Chem. Phys.
Discussion started: 14 November 2017


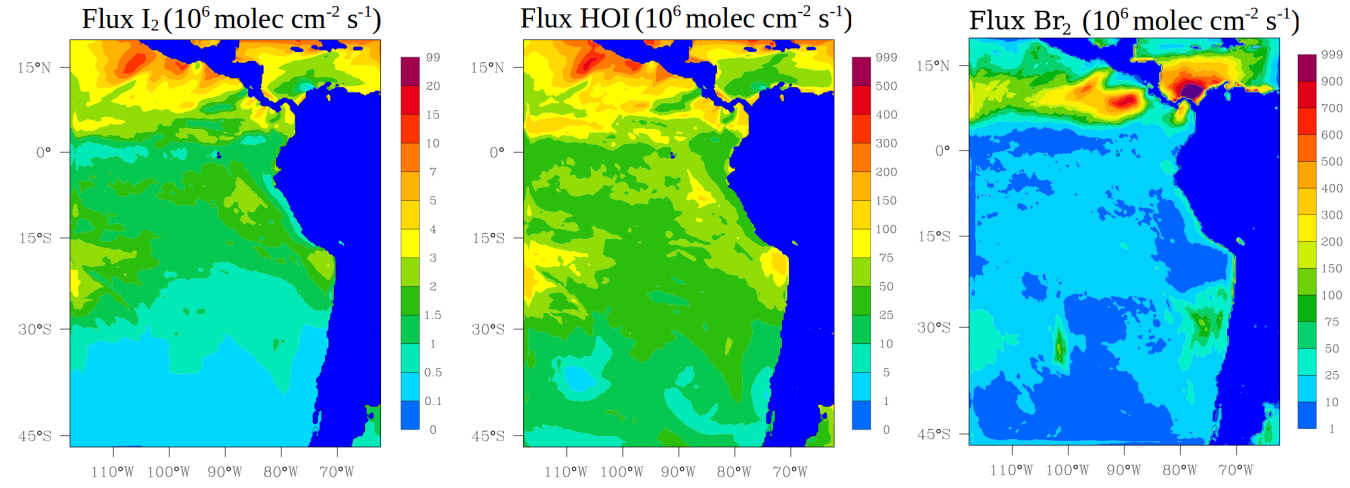


**Figure 2.** Mean oceanic surface fluxes for inorganic iodine: $I_2$ (left panel) and HOI (middle panel). The column-integrated fluxes for inorganic bromine ($Br_2$, right panel) from the debromination process during January and February 2012 are also shown. Values are given in $10^6$ molec $cm^{-2}$ $s^{-1}$.

Atmos. Chem. Phys. Discuss., https://doi.org/10.5194/acp-2017-903
Manuscript under review for journal Atmos. Chem. Phys.
Discussion started: 14 November 2017


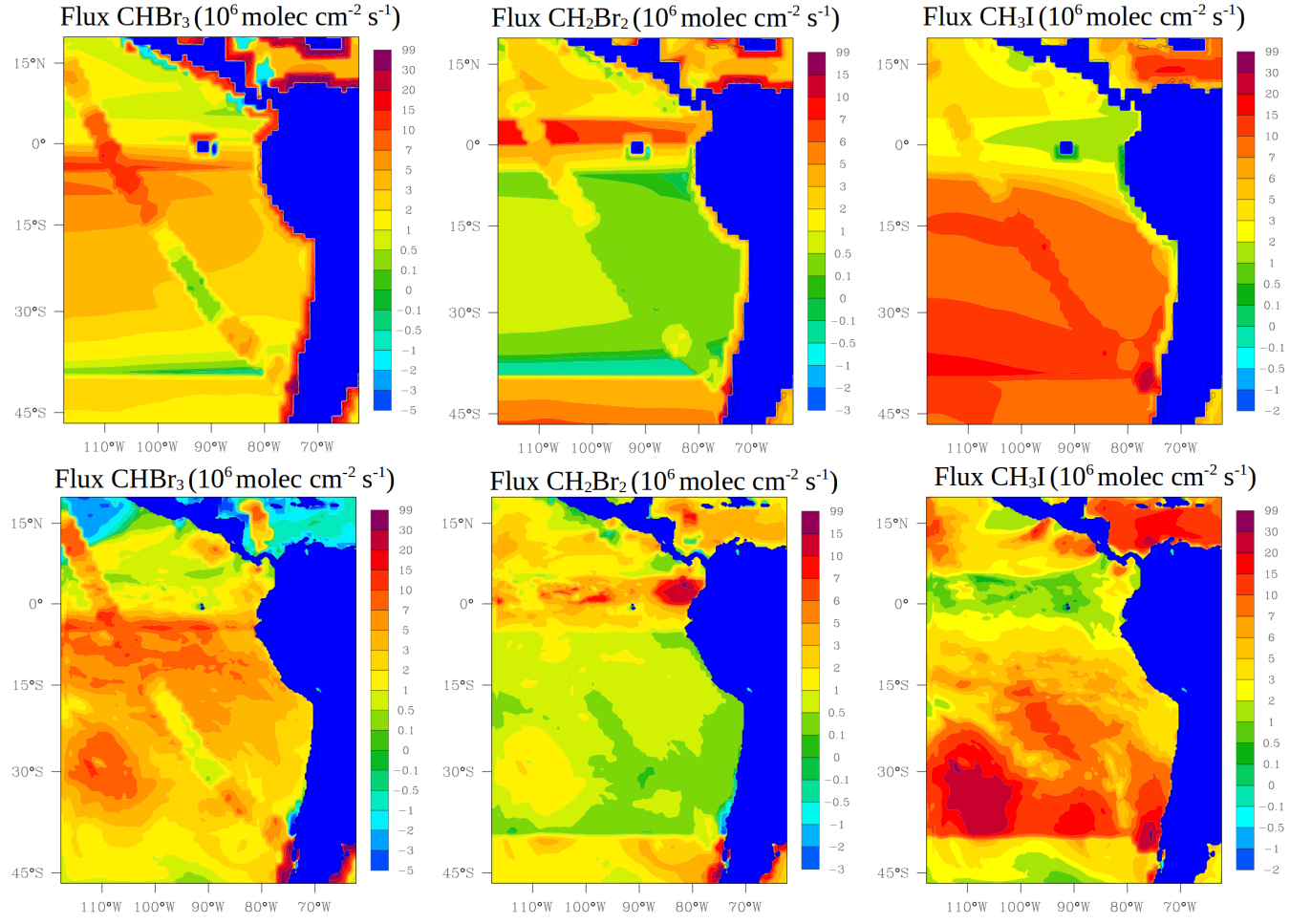


**Figure 3.** Mean oceanic fluxes for halocarbons ($CHBr_3$, $CH_2Br_2$ and $CH_3I$) during January and February 2012. Prescribed fluxes are shown on the top and online fluxes on the bottom. Values are given in $10^6$ molec $cm^{-2}$ $s^{-1}$.

Atmos. Chem. Phys. Discuss., https://doi.org/10.5194/acp-2017-903
Manuscript under review for journal Atmos. Chem. Phys.
Discussion started: 14 November 2017


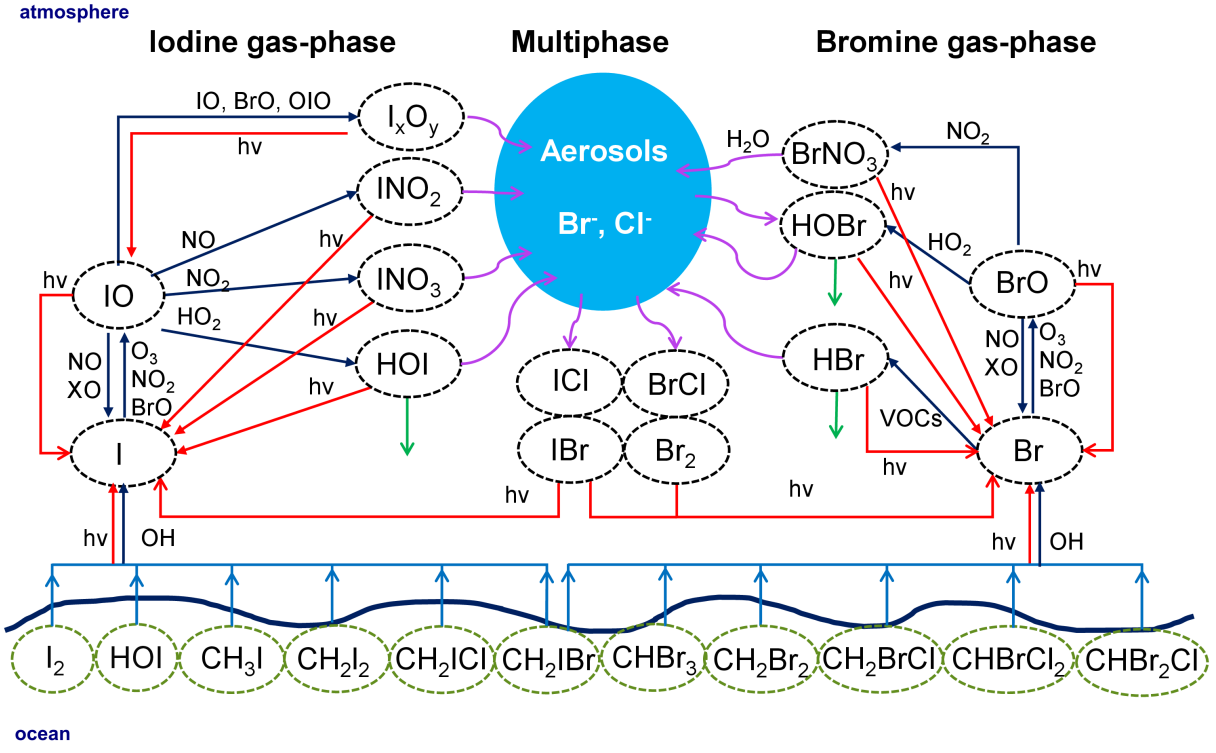


**Figure 4.** Schematic representation of the implemented iodine and bromine chemistry in WRF-Chem. Red lines represent photolytic reactions, dark blue lines gas-phase pathways, light blue lines fluxes, green lines deposition and purple curved lines heterogeneous pathways.

Atmos. Chem. Phys. Discuss., https://doi.org/10.5194/acp-2017-903
Manuscript under review for journal Atmos. Chem. Phys.
Discussion started: 14 November 2017


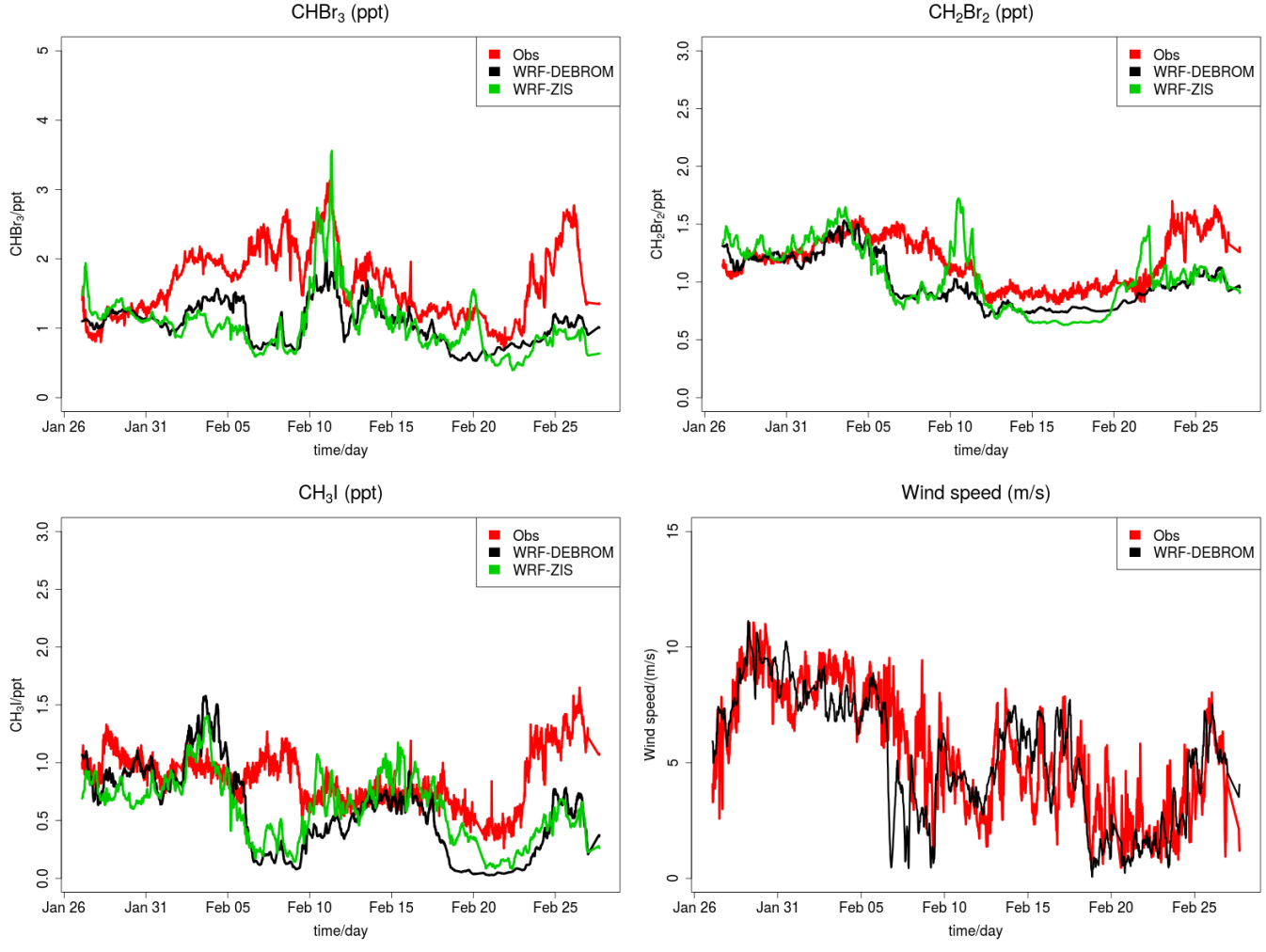


**Figure 5.** Time series of $CHBr_3$ (top left), $CH_2Br_2$ (top right) and $CH_3I$ (bottom left) mixing rations (in ppt) for the WRF-ZIS (green line) and WRF-DEBROM (black line) runs during the period of the TORERO campaign in 2012. On the bottom-right, the wind speed (m $s^{-1}$) of the model is shown with a black line. Measurements during the TORERO campaign are depicted with red lines.

Atmos. Chem. Phys. Discuss., https://doi.org/10.5194/acp-2017-903
Manuscript under review for journal Atmos. Chem. Phys.
Discussion started: 14 November 2017


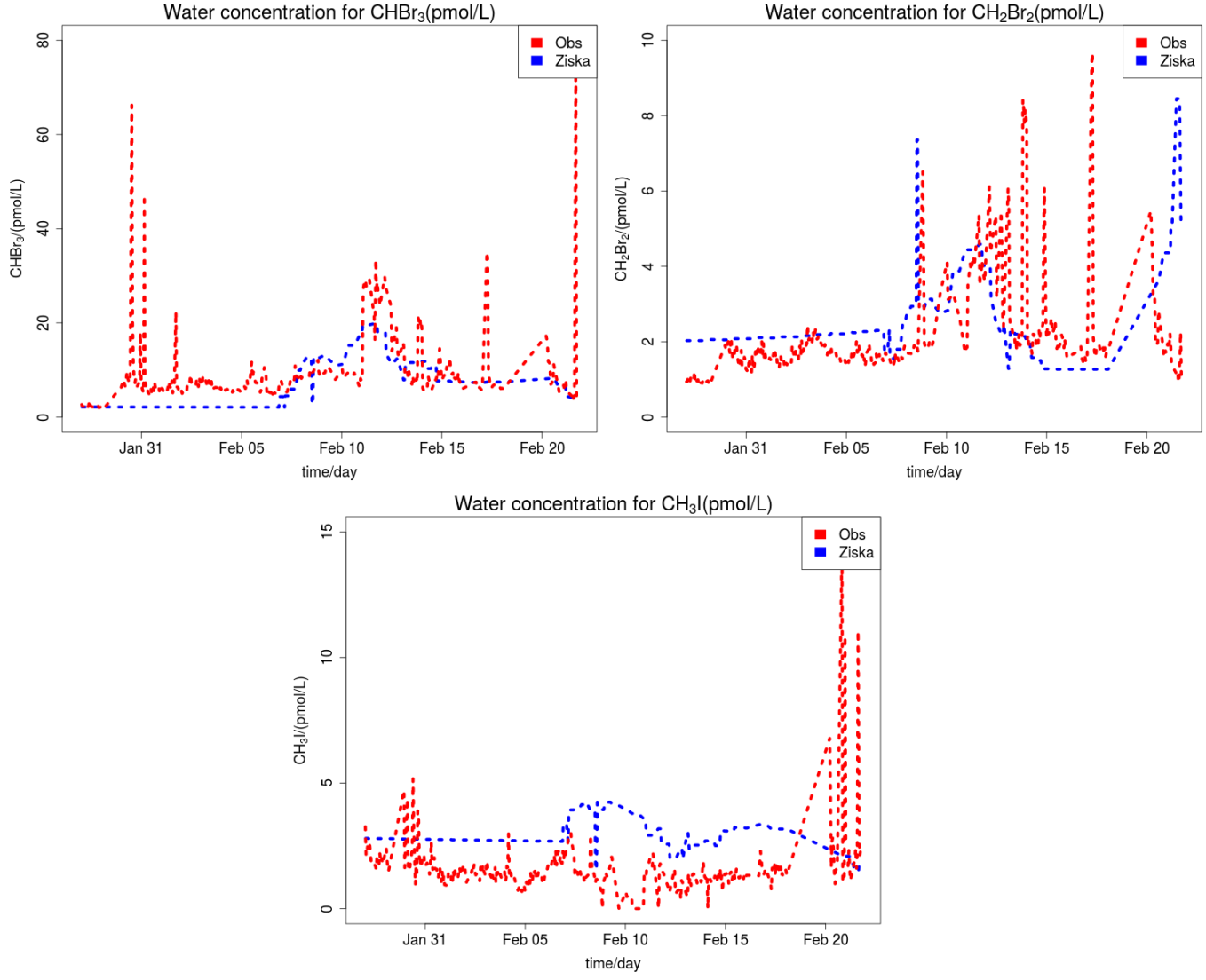


**Figure 6.** Time series of measured $CHBr_3$ (top left), $CH_2Br_2$ (top right) and $CH_3I$ (bottom) water concentration (in pmol/L) during the TORERO campaign (red dashed line) and from the Ziska et al. (2013) climatology (blue dashed line).

Atmos. Chem. Phys. Discuss., https://doi.org/10.5194/acp-2017-903
Manuscript under review for journal Atmos. Chem. Phys.
Discussion started: 14 November 2017


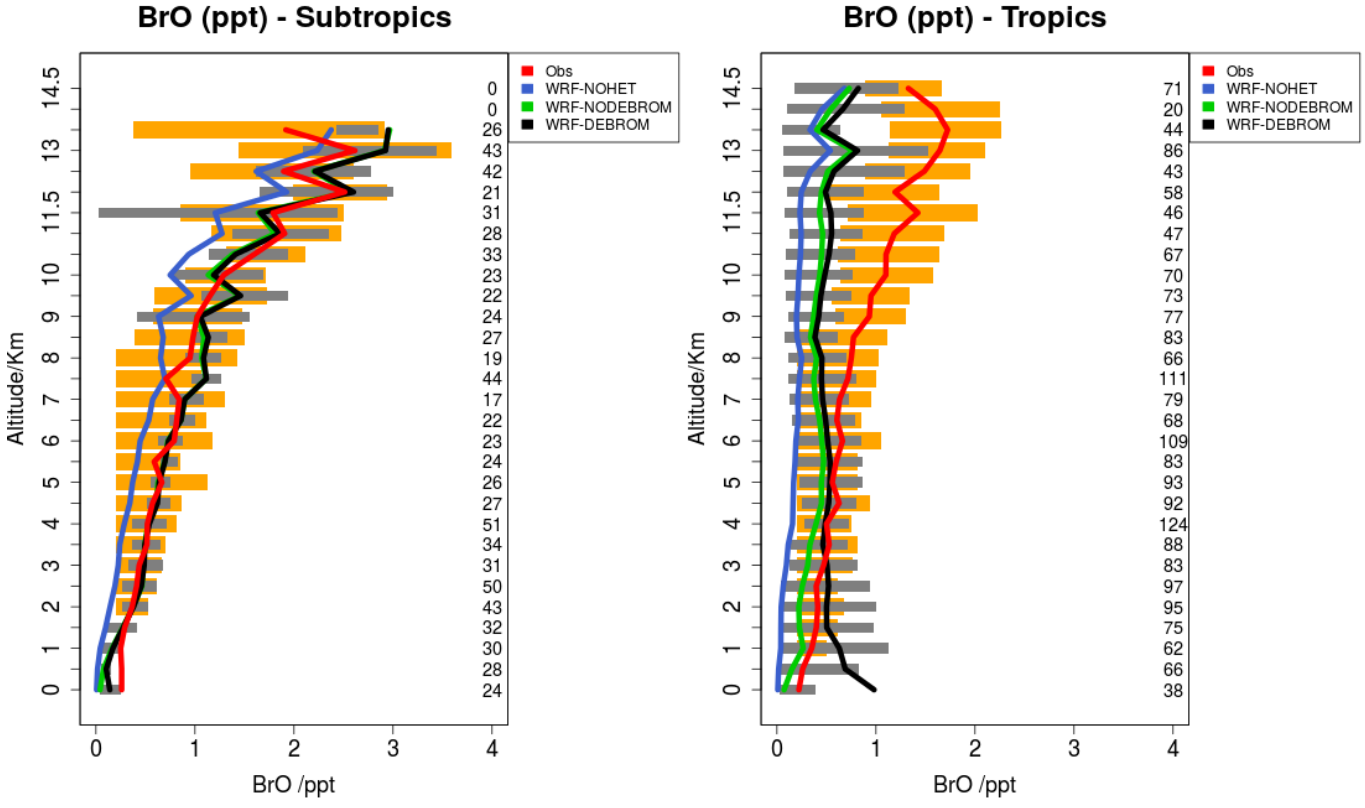


**Figure 7.** Mean vertical profile of BrO (ppt) over the subtropics (left) and tropics (right). An average over 16 flights of the TORERO campaign (red line) are compared to the 3 different WRF-Chem simulations: WRF-NOHET (blue line), WRF-NODEBROM (green line) and WRF-DEBROM (black line). Orange and grey horizontal bars indicate the 25th-75th quartile interval for the observations of the TORERO campaign and WRF-DEBROM simulation, respectively. Values are considered in 0.5 km bins and the aircraft measurement points for each altitude is given on the right side of each plot.

Atmos. Chem. Phys. Discuss., https://doi.org/10.5194/acp-2017-903
Manuscript under review for journal Atmos. Chem. Phys.
Discussion started: 14 November 2017


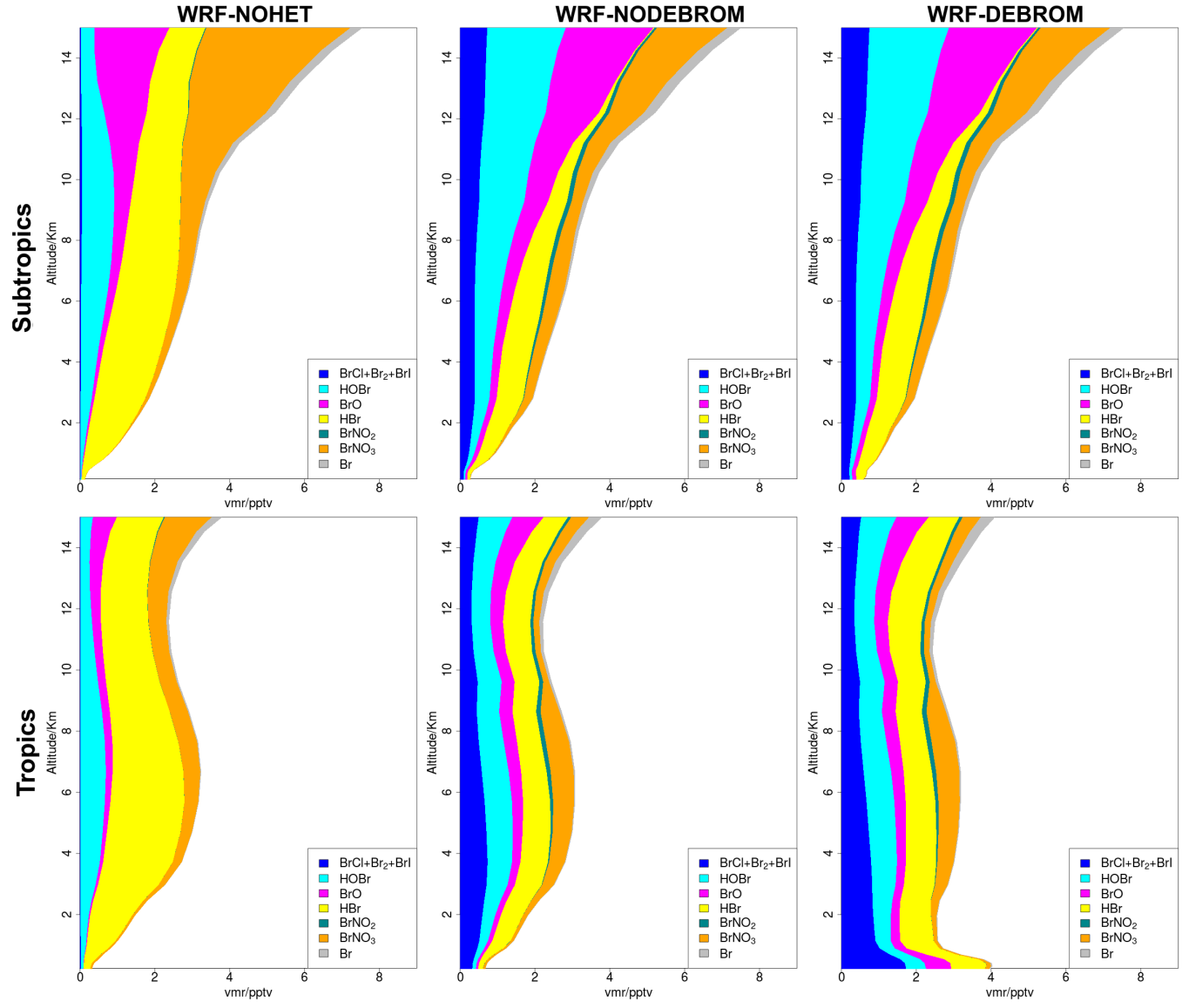


**Figure 8.** Regional average vertical partitioning of inorganic bromine ($Br_y$) for the three different simulations WRF-NOHET (left panel), WRF-NODEBROM (middle panel) and WRF-DEBROM (right panel) during January and February 2012. Top panels are over the tropical area and bottom panels over the subtropical. Units are in ppt.

Atmos. Chem. Phys. Discuss., https://doi.org/10.5194/acp-2017-903
Manuscript under review for journal Atmos. Chem. Phys.
Discussion started: 14 November 2017


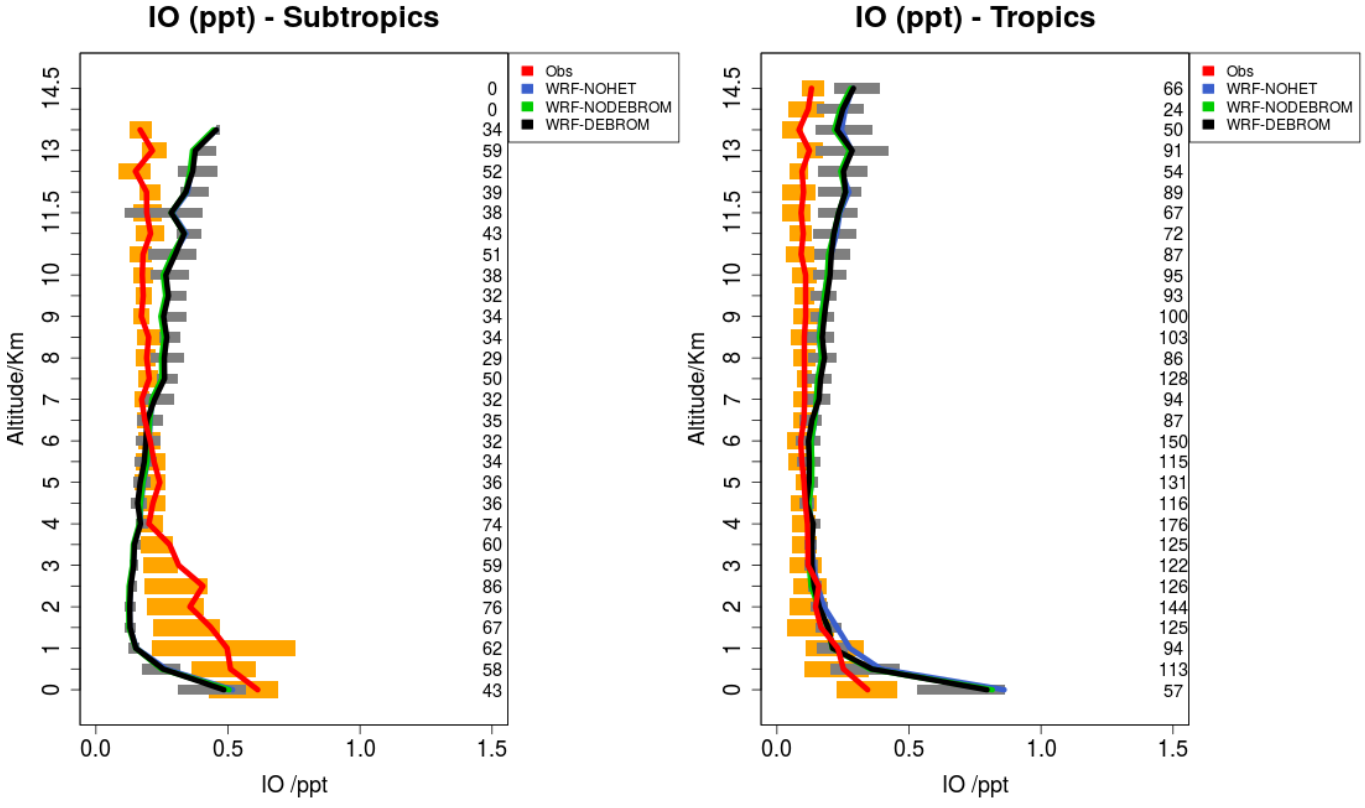


**Figure 9.** Mean vertical profile of IO (ppt) over the subtropics (left) and tropics (right). An average over 16 flights of the TORERO campaign (red line) are compared to the 3 different WRF-Chem simulations: WRF-NOHET (blue line), WRF-NODEBROM (green line) and WRF-DEBROM (black line). Orange and grey horizontal bars indicate the 25th-75th quartile interval for the observations of the TORERO campaign and WRF-DEBROM simulation, respectively. Values are considered in 0.5 km bin and the aircraft measurement points for each altitude is given on the right side of each plot.

Atmos. Chem. Phys. Discuss., https://doi.org/10.5194/acp-2017-903
Manuscript under review for journal Atmos. Chem. Phys.
Discussion started: 14 November 2017


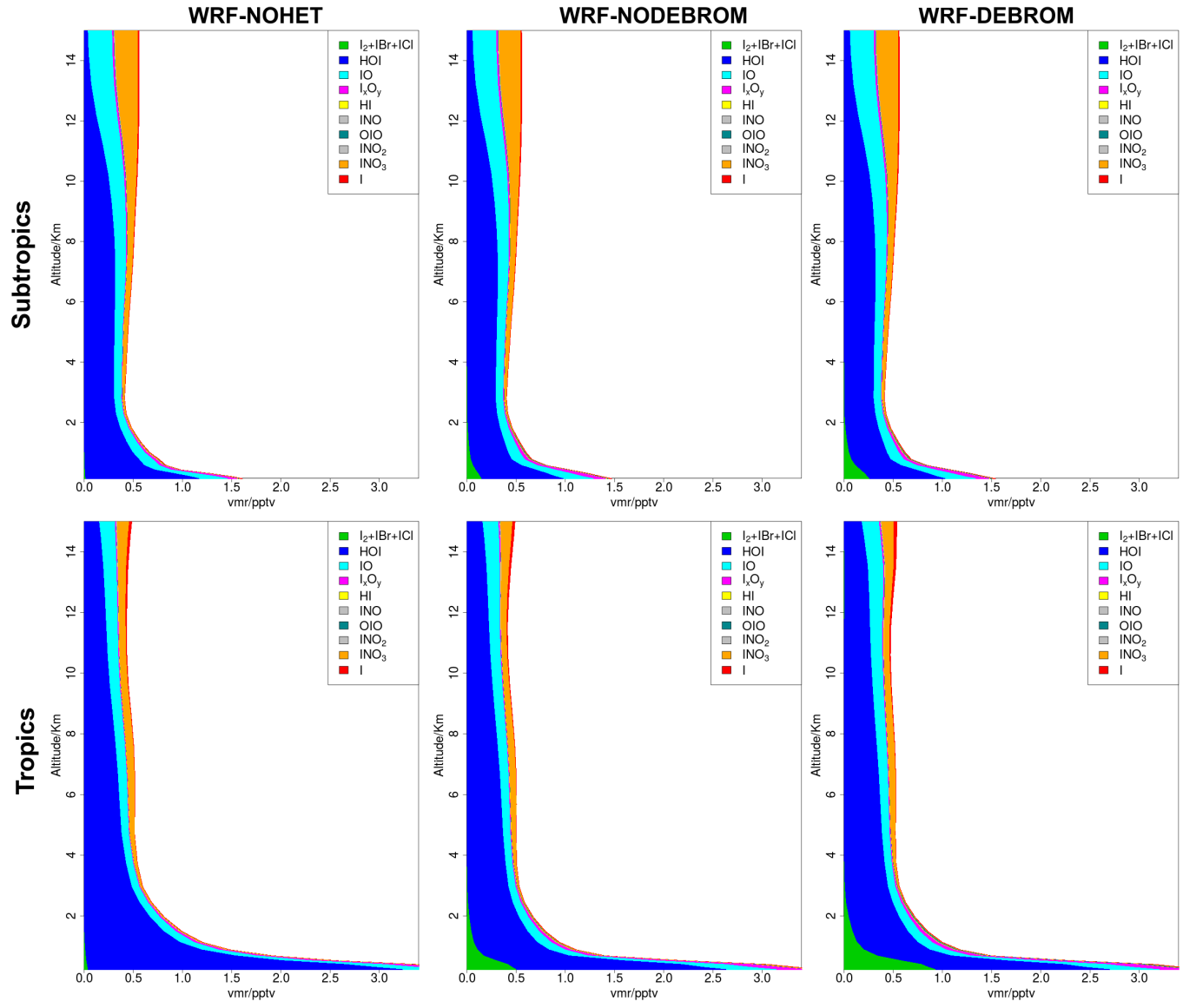


**Figure 10.** Regional average vertical partitioning of inorganic iodine ($I_y$)) for the three different simulations WRF-NOHET (left panel), WRF-NODEBROM (middle panel) and WRF-DEBROM (right panel) during January and February 2012. Top panels are over the tropical area and bottom panels over the subtropical. Units are in ppt.

Atmos. Chem. Phys. Discuss., https://doi.org/10.5194/acp-2017-903
Manuscript under review for journal Atmos. Chem. Phys.
Discussion started: 14 November 2017


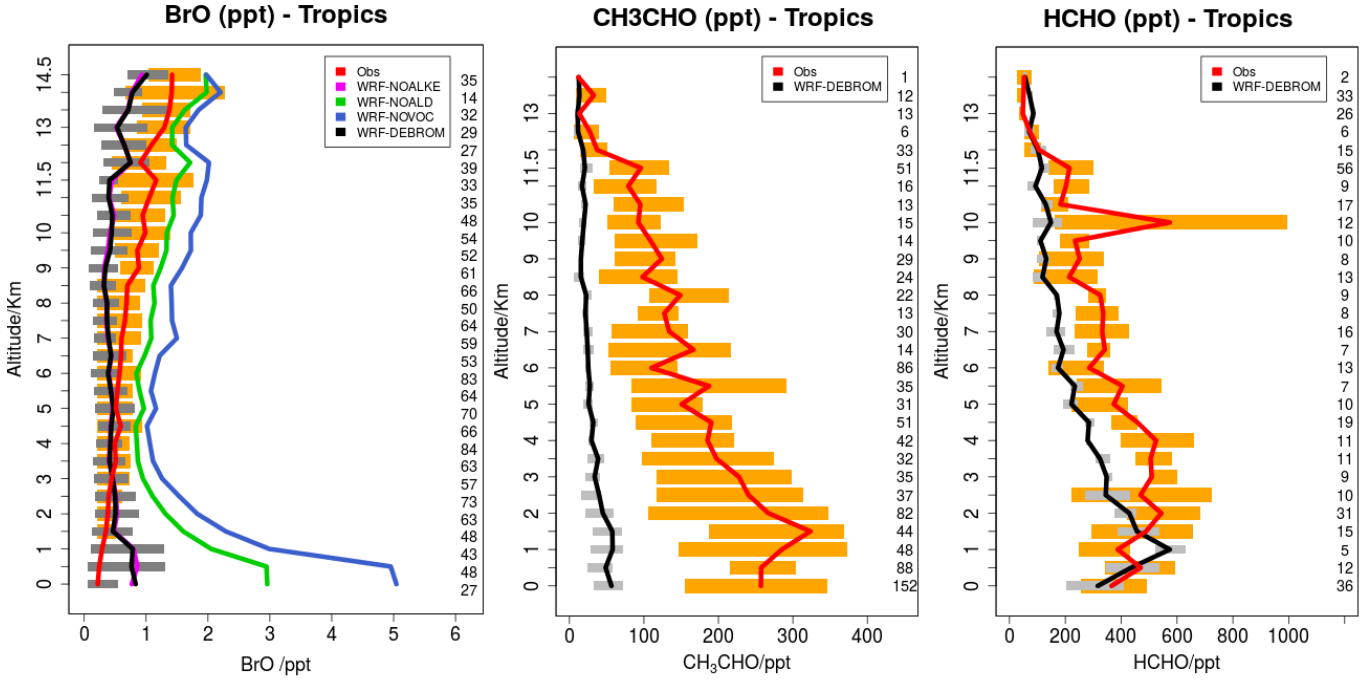


**Figure 11.** Mean vertical profile of BrO (ppt) over the tropics in the left panel. A sub-set of 9 flights from the TORERO campaign (red line) are compared to the 4 different WRF-Chem simulations: WRF-NOALKE (blue line), WRF-NOALD (green line), WRF-NOVOCS (blue line) and WRF-DEBROM (black line). In the middle and right panel, the WRF-DEBROM (black line) simulation is compared with acetaldehyde and formaldehyde TORERO observations for the same 9 flights (red line). Orange and grey horizontal bars indicate the 25th-75th quartile interval for the observations of the TORERO campaign and WRF-DEBROM simulation, respectively. Values are considered in 0.5 km bin and the number of points for each altitude is given on the right side of each plot. Units are in ppt.

Atmos. Chem. Phys. Discuss., https://doi.org/10.5194/acp-2017-903
Manuscript under review for journal Atmos. Chem. Phys.
Discussion started: 14 November 2017


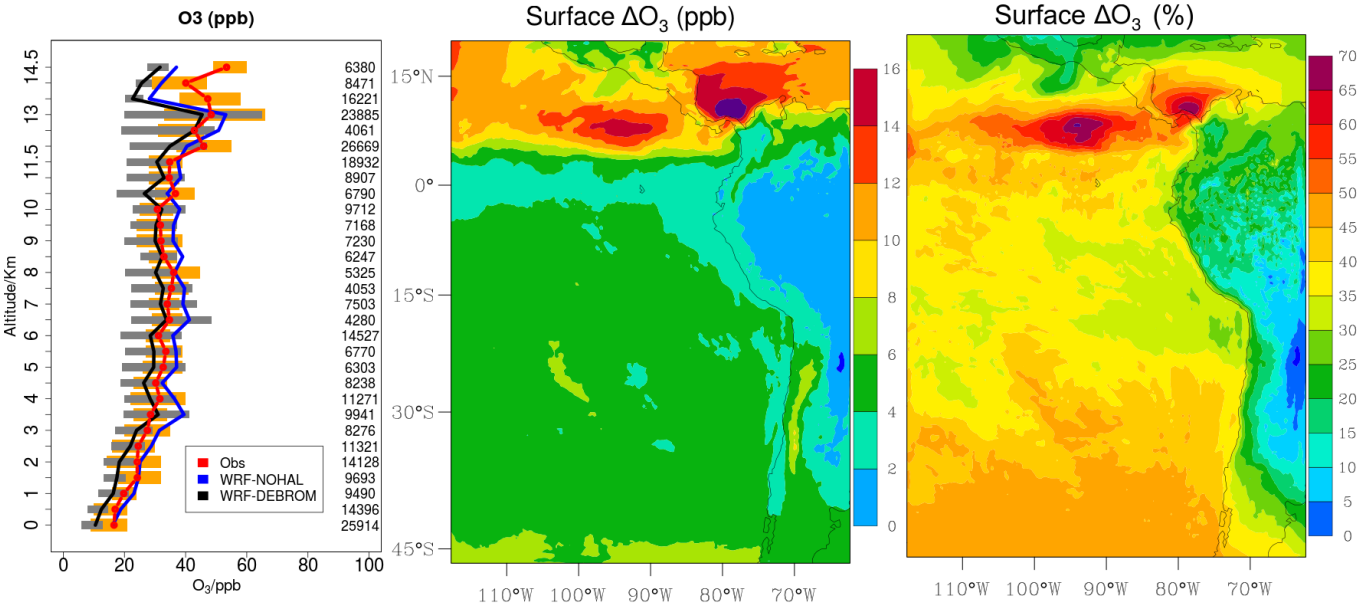


**Figure 12.** On the left, mean vertical profile of $O_3$ (ppb) over the domain area using 13 flights from the TORERO campaign (red line) are compared to the 2 different WRF-Chem simulations: WRF-NOHAL (blue line) and WRF-DEBROM (black line). Orange and grey horizontal bars indicate the 25th-75th quartile interval for the observations of the TORERO campaign and WRF-DEBROM simulation, respectively. Values are considered in 0.5 km bins and the aircraft measurement points for each altitude is given on the right side of each plot. On the middle and right, mean $O_3$ difference between the simulation with no halogen chemistry (WRF-NOHAL) and with halogen chemistry (WRF-DEBROM) for January and February 2012. Surface mean bias (ppb) is shown in the left panel and surface relative mean bias (%) in the right panel. Relative mean bias (%) is calculated as (WRF-NOHAL - WRF-DEBROM)/WRF-NOHAL × 100.

Atmos. Chem. Phys. Discuss., https://doi.org/10.5194/acp-2017-903
Manuscript under review for journal Atmos. Chem. Phys.
Discussion started: 14 November 2017


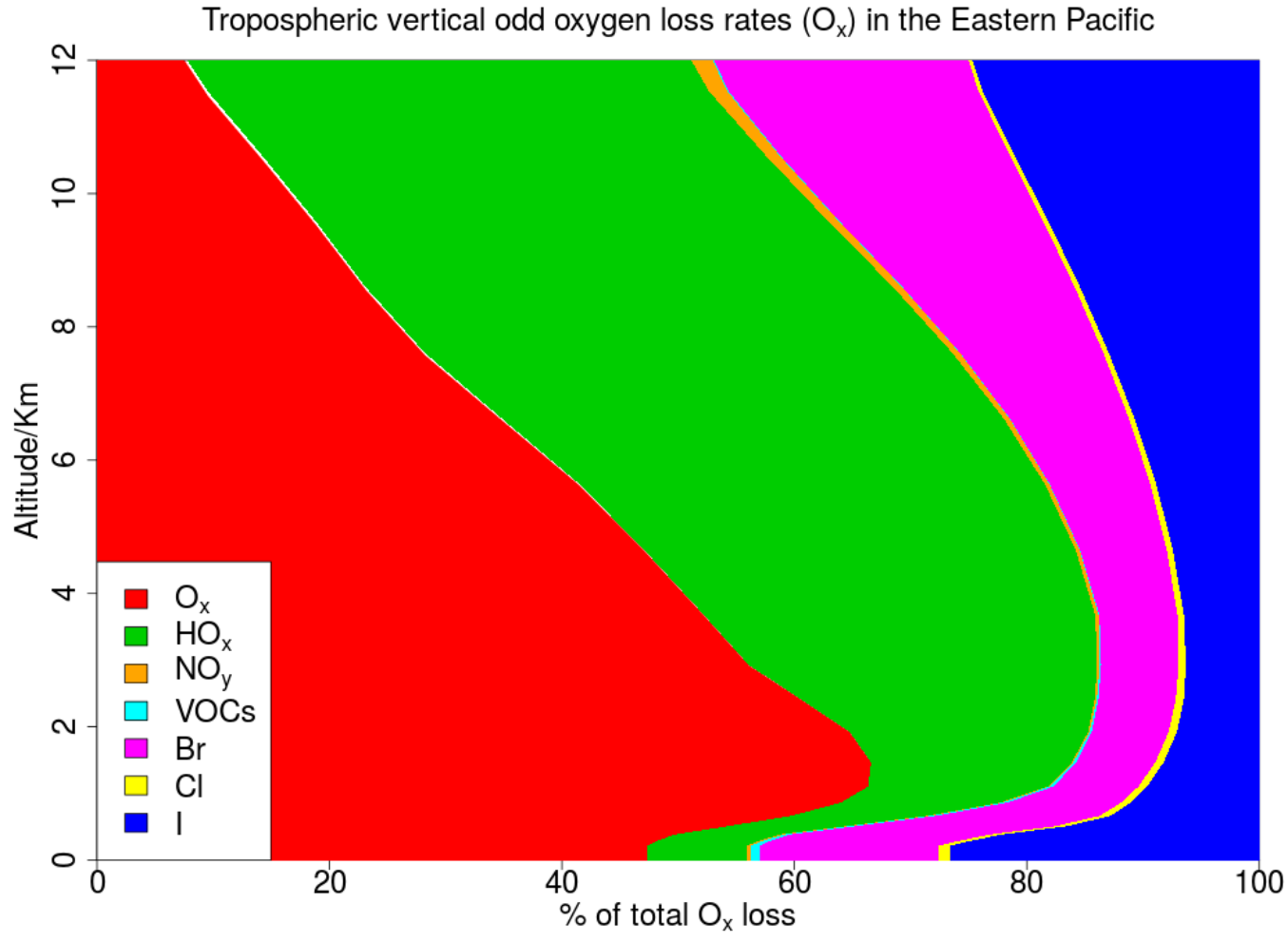


**Figure 13.** Regional average percentage contribution of each ozone depleting family to the total tropospheric vertical odd oxygen loss ($O_x$) for the WRF-DEBROM simulation.

Atmos. Chem. Phys. Discuss., https://doi.org/10.5194/acp-2017-903
Manuscript under review for journal Atmos. Chem. Phys.
Discussion started: 14 November 2017


Atmospheric Chemistry and Physics Discussions

**Table 1.** Henry's Law constant for relevant halogen species implemented in WRF-Chem. $INO_2$ Henry's law constant is assumed equal to that of $BrNO_2$. Iodine oxides ( $I_2O_X$ ) Henry's law constants are assumed to be infinity by analogy with $INO_3$. Virtually infinity solubility is represented by using a very large number ($2.69\times10^{15}$).

| Species | Henry's Law Constant (H) at 298K (M $atm^{-1}$) | $\frac{d(lnH)}{d(1/T)}$ (K) | Reference |
|---|---|---|---|
| $ClNO_3$ | $\infty$ | - | Sander (2015) |
| $BrNO_3$ | $\infty$ | - | Sander (2015) |
| $INO_3$ | $\infty$ | - | Sander et al. (2006) |
| HOCl | $6.5\times10^{2}$ | 5900 | Sander (2015) |
| HOBr | $1.9\times10^{3}$ | - | Sander (2015) |
| HOI | $4.5\times10^{2}$ | - | Sander et al. (2011a) |
| HCl[a] | $7.1\times10^{15}$ | 5900 | Sander (2015) |
| HBr[a] | $7.5\times10^{13}$ | 10200 | Frenzel et al. (1998); Schweitzer et al. (2000) |
| HI[a] | $7.43\times10^{13}$ | 3190 | Sander (2015); Sander et al. (2006) |
| BrCl | 0.9 | 5600 | Sander (2015) |
| IBr | $2.4\times10^{1}$ | - | Sander (2015) |
| ICl | $1.1\times10^{2}$ | - | Sander (2015) |
| $BrNO_2$ | $3.\times10^{-1}$ | - | Sander (2015) |
| $ClNO_2$ | $4\times10^{-2}$ | - | Sander (2015) |
| $INO_2$ | $3.\times10^{-1}$ | - | see caption text |
| $I_2$ | 2.63 | 4600 | Sander (2015) |
| $Br_2$ | 0.8 | 4000 | Sander (2015) |
| $I_2O_2$ | $\infty$ | - | see caption text |
| $I_2O_3$ | $\infty$ | - | see caption text |
| $I_2O_4$ | $\infty$ | - | see caption text |

[a] Effective Henry's law of HX is calculated for acid conditions (pH = 4.5): $K_H^*(T) = K_H(T) \times (1 + \frac{K_a}{[H^+]})$, where X= Cl, I or Br and $K_a = 1 \times 10^9$M is the acid dissociation constant (Bell, 1973).

Atmos. Chem. Phys. Discuss., https://doi.org/10.5194/acp-2017-903
Manuscript under review for journal Atmos. Chem. Phys.
Discussion started: 14 November 2017


Atmospheric Chemistry and Physics Discussions

**Table 2.** Bimolecular and thermal decomposition halogen reactions included in WRF-Chem. These reactions are given in the Arrhenius form with the rate equal to $A \times e^{\frac{-Ea}{RT}}$.

| Reactions | A ($cm^3$ $molecules^{-1}$ $s^{-1}$) | $\frac{Ea}{R}$ (K) | Reference |
|---|---|---|---|
| $Cl + O_3 \rightarrow ClO + O_2$ | $2.8\times10^{-11}$ | 250 | Atkinson et al. (2007) |
| $Cl + HO_2 \rightarrow HCL + O_2$ | $7.8\times10^{-11}$ | 620 | Atkinson et al. (2007) |
| $Cl + HO_2 \rightarrow CLO + OH$ | $7.8\times10^{-11}$ | 620 | Atkinson et al. (2007) |
| $Cl + H_2O_2 \rightarrow HCl + HO_2$ | $1.1\times10^{-11}$ | 980 | Atkinson et al. (2007) |
| $Cl + H_2 + O_2 \rightarrow HCl + HO_2$ | $3.9\times10^{-11}$ | 2310 | Atkinson et al. (2007) |
| $ClO + OH \rightarrow Cl + HO_2$ | $6.8\times10^{-12}$ | -300 | Atkinson et al. (2007) |
| $ClO + OH \rightarrow HCl$ | $4.38\times10^{-13}$ | -300 | Atkinson et al. (2007) |
| $ClO + HO_2 \rightarrow HOCl$ | $2.2\times10^{-12}$ | -340 | Atkinson et al. (2007) |
| $ClO + O_3 \rightarrow Cl + 2O_2$ | $1.5\times10^{-17}$ | - | Atkinson et al. (2007) |
| $ClO + NO \rightarrow Cl + NO_2$ | $6.2\times10^{-12}$ | -295 | Atkinson et al. (2007) |
| $HCl + OH \rightarrow Cl + H_2O$ | $1.7\times10^{-12}$ | 230 | Atkinson et al. (2007) |
| $HOCl + OH \rightarrow ClO + H_2O$ | $3.0\times10^{-12}$ | 500 | Burkholder et al. (2015) |
| $Cl + ClNO_3 \rightarrow Cl_2 + NO_3$ | $6.2\times10^{-12}$ | -145 | Atkinson et al. (2007) |
| $ClNO_3 + OH \rightarrow 0.5ClO + 0.5HNO_3 + 0.5HOCl + 0.5NO_3$ | $1.2\times10^{-12}$ | 330 | Atkinson et al. (2007) |
| $ClNO_2 + OH \rightarrow HOCl + NO_2$ | $2.4\times10^{-12}$ | 1250 | Sander et al. (2011b) |
| $ClO + ClO \rightarrow Cl_2 + O_2$ | $1.0\times10^{-12}$ | 1590 | Sander et al. (2011b) |
| $ClO + ClO \rightarrow OClO + Cl$ | $3.5\times10^{-13}$ | 1370 | Sander et al. (2011b) |
| $ClO + ClO \rightarrow 2Cl$ | $3.0\times10^{-11}$ | 2450 | Sander et al. (2011b) |
| $Cl + CH_4 \rightarrow HCl + CH_3O_2$ | $6.6\times10^{-12}$ | 1240 | Atkinson et al. (2006) |
| $Cl + CH_2O \rightarrow HCl + HO_2 + CO$ | $8.1\times10^{-11}$ | 34 | Atkinson et al. (2006) |
| $Cl + CH_3CHO \rightarrow HCl + CH_3CO_3$ | $8.0\times10^{-11}$ | - | Atkinson et al. (2006) |
| $Cl + CH_3OH \rightarrow HCl + HO_2 + CH_2O$ | $5.5\times10^{-11}$ | - | Atkinson et al. (2006) |
| $Cl + CH_3OOH \rightarrow HCl + CH_3O_2 + OH$ | $5.7\times10^{-11}$ | - | Atkinson et al. (2006) |
| $Cl + CH_3O_2 \rightarrow 0.5CH_2O + 0.5CO + 0.5H_2O + 0.5HO_2 + 0.5HCl + 0.5ClO$ | $1.6\times10^{-10}$ | - | Burkholder et al. (2015) |
| $ClO + CH_3O_2 \rightarrow Cl + CH_2O + HO_2$ | $3.3\times10^{-12}$ | 115 | Atkinson et al. (2008) |
| $Cl + C_2H_6 (+ O_2) \rightarrow HCl + C_2H_5O_2$ | $7.2\times10^{-11}$ | 70 | Sander et al. (2011b) |
| $Cl + C_3H_8 (+ O_2) \rightarrow HCl + C_3H_7O_2$ | $7.85\times10^{-11}$ | 80 | Sander et al. (2011b) |
| $Cl + C_3H_6 (+ O_2) \rightarrow HCl + PO2$ | $3.6\times10^{-12}$ | | Sander et al. (2011b) |
| $CH_3Cl + Cl \rightarrow HO_2 + CO + 2HCl$ | $3.20\times10^{-11}$ | 1250 | Sander et al. (2011b) |
| $CH_3Cl + OH \rightarrow Cl + H_2O + HO_2$ | $2.40\times10^{-12}$ | 12509 | Sander et al. (2011b) |

Atmos. Chem. Phys. Discuss., https://doi.org/10.5194/acp-2017-903
Manuscript under review for journal Atmos. Chem. Phys.
Discussion started: 14 November 2017


Atmospheric Chemistry and Physics Discussions

Table 2: Continued from previous page

| Reactions | A ($cm^3$ $molecules^{-1}$ $s^{-1}$) | $\frac{Ea}{R}$ (K) | Reference |
|---|---|---|---|
| $Br + O_3 \rightarrow BrO + O_2$ | $1.7\times10^{-11}$ | 800 | Atkinson et al. (2007) |
| $Br + HO_2 \rightarrow HBr + O_2$ | $7.7\times10^{-12}$ | 450 | Atkinson et al. (2007) |
| $BrO + OH \rightarrow Br + HO_2$ | $1.8\times10^{-11}$ | -250 | Atkinson et al. (2007) |
| $BrO + HO_2 \rightarrow HOBr + O_2$ | $4.5\times10^{-12}$ | -500 | Atkinson et al. (2007) |
| $BrO + NO \rightarrow Br + NO_2$ | $8.7\times10^{-12}$ | -260 | Atkinson et al. (2007) |
| $BrO + BrO \rightarrow 2Br + O_2$ | $2.4\times10^{-12}$ | -40 | Sander et al. (2011b) |
| $BrO + BrO \rightarrow Br_2 + O_2$ | $2.8\times10^{-14}$ | -840 | Sander et al. (2011b) |
| $HBr + OH \rightarrow Br + H_2O$ | $6.7\times10^{-12}$ | -155 | Atkinson et al. (2007) |
| $BrNO_3 + Br \rightarrow Br_2 + NO_3$ | $4.9\times10^{-11}$ | - | Orlando and Tyndall (1996) |
| $Br + NO_3 \rightarrow BrO + NO_2$ | $1.6\times10^{-11}$ | - | Sander et al. (2011b) |
| $Br_2 + OH \rightarrow HOBr + Br$ | $2.1\times10^{-11}$ | -240 | Sander et al. (2011b) |
| $Br + CH_2O \rightarrow HBr + CO + HO_2$ | $1.7\times10^{-11}$ | 800 | Sander et al. (2011b)) |
| $Br + CH_3CHO \rightarrow HBr + CH_3CO_3$ | $1.8\times10^{-11}$ | 460 | Atkinson et al. (2006) |
| $Br + C_2H_4 (+ O_2) \rightarrow BrRO_2$ | $1.3\times10^{-13}$ | - | Atkinson et al. (2006) |
| $Br + C_3H_6 (+ O_2) \rightarrow BrRO_2$ | $3.6\times10^{-12}$ | - | Atkinson et al. (2006) |
| $BrRO_2 + NO \rightarrow 0.2\ HBr + 0.8\ Br + CH_3CO_3 + NO_2 + 0.5\ CH_2O + HO_2$ | $4.06\times10^{-12}$ | -360 | Toyota et al. (2004) |
| $BrRO_2 + CH_3O_2 \rightarrow 0.2\ HBr + 0.8\ Br + CH_3CO_3 + HO_2 + CH_2O$ | $1.48\times10^{-12}$ | - | Toyota et al. (2004) |
| $BrRO_2 + HO_2 \rightarrow BrOR + H_2O$ | $7.5\times10^{-12}$ | - | Toyota et al. (2004) |
| $CH_3Br + OH \rightarrow Br + H_2O + HO_2$ | $2.35\times10^{-12}$ | 1300 | Sander et al. (2006) |
| $CH_2Br_2 + OH \rightarrow 2Br$ | $2.0\times10^{-12}$ | 840 | Sander et al. (2006) |
| $CH_2BrCl + OH \rightarrow Br + Cl$ | $2.4\times10^{-12}$ | 920 | Sander et al. (2006) |
| $CHBrCl_2 + OH \rightarrow Br + 2Cl$ | $9.0\times10^{-13}$ | 600 | Sander et al. (2006) |
| $CHBr_2Cl + OH \rightarrow 2Br + Cl$ | $9.0\times10^{-13}$ | 600 | Sander et al. (2006) |
| $CHBr_3 + OH \rightarrow 3Br$ | $1.35\times10^{-12}$ | 600 | Sander et al. (2006) |
| $I + O_3 \rightarrow IO (+ O_2)$ | $2.1\times10^{-11}$ | 830 | Atkinson et al. (2007) |
| $I + HO_2 \rightarrow HI (+ O_2)$ | $1.5\times10^{-11}$ | 1090 | Atkinson et al. (2007) |
| $I + NO_3 \rightarrow IO + NO_2$ | $1.0\times10^{-10}$ | - | Atkinson et al. (2007) |
| $I_2 + OH \rightarrow HOI + I$ | $1.8\times10^{-10}$ | - | Burkholder et al., (2015) |
| $IO + HO_2 \rightarrow HOI (+ O_2)$ | $1.4\times10^{-11}$ | -540 | Atkinson et al. (2007) |
| $IO + NO \rightarrow I + NO_2$ | $7.15\times10^{-12}$ | -300 | Atkinson et al. (2007) |
| $IO + IO \rightarrow I + OIO$ | $2.16\times10^{-11}$ | -180 | Atkinson et al. (2007) |
| $IO + IO \rightarrow I_2O_2$ | $3.24\times10^{-11}$ | -180 | Atkinson et al. (2007) |
| $OIO + NO \rightarrow NO_2 + IO$ | $1.1\times10^{-12}$ | -542 | Atkinson et al. (2007) |

Atmos. Chem. Phys. Discuss., https://doi.org/10.5194/acp-2017-903
Manuscript under review for journal Atmos. Chem. Phys.
Discussion started: 14 November 2017


Atmospheric Chemistry and Physics Discussions

Table 2: Continued from previous page

| Reactions | A ($cm^3$ $molecules^{-1}$ $s^{-1}$) | $\frac{Ea}{R}$ (K) | Reference |
|---|---|---|---|
| OIO + OIO → $I_2O_4$ | $1.5\times10^{-10}$ | - | Gómez Martín et al. (2007) |
| IO + OIO → $I_2O_3$ | $1.5\times10^{-10}$ | - | Gómez Martín et al. (2007) |
| $I_2O_2$ → IO + IO | $1\times10^{-12}$ | 9770 | Ordóñez et al. (2012) |
| $I_2O_2$ → OIO + I | $2.5\times10^{-14}$ | 9770 | Ordóñez et al. (2012) |
| $I_2O_4$ → 2OIO | $3.8\times10^{-2}$ | - | Kaltsoyannis and Plane 2008 |
| HI + OH → I + $H_2O$ | $1.6\times10^{-11}$ | -440 | Atkinson et al. (2007) |
| HOI + OH → IO + $H_2O$ | $5.0\times10^{-12}$ | - | Riffault et al., 2005 |
| $INO_2$ (+M) → I + $NO_2$ | $9.94\times10^{17}$ | 11859 | McFiggans et al. (2000) |
| $INO_3$ → IO + $NO_2$ | $1.1\times10^{15}$ | 12060 | Atkinson et al. (2007) |
| INO + INO → $I_2$ + 2NO | $8.4\times10^{-11}$ | 2620 | Atkinson et al. (2007) |
| $INO_2$ + $INO_2$ → $I_2$ + 2$NO_2$ | $4.7\times10^{-12}$ | 1670 | Atkinson et al. (2007) |
| $I_2$ + $NO_3$ → I + $INO_3$ | $1.5\times10^{-12}$ | | Atkinson et al. (2007) |
| $INO_3$ + I → $I_2$ + $NO_3$ | $9.1\times10^{-11}$ | 146 | Kaltsoyannis and Plane 2008 |
| IO + $CH_3O_2$ + $O_2$ → $CH_2O$ + $HO_2$ + I + 0.5$O_2$ | $2.0\times10^{-12}$ | - | Dillon et al., 2006 |
| I + BrO → IO + Br | $1.2\times10^{-11}$ | - | Sander et al. (2011b) |
| IO + Br → I + BrO | $2.7\times10^{-11}$ | - | Bedjanina et al. 1997 |
| BrO + ClO → Br + OClO | $1.6\times10^{-12}$ | -430 | Atkinson et al. (2007) |
| BrO + ClO → Br + Cl + $O_2$ | $2.9\times10^{-12}$ | -220 | Atkinson et al. (2007) |
| BrO + ClO → BrCl + $O_2$ | $5.8\times10^{-13}$ | -170 | Atkinson et al. (2007) |
| IO + ClO → 0.33ICl + 0.67I + 0.33Cl + 0.33OClO + 0.67$O_2$ | $9.4\times10^{-13}$ | -280 | Atkinson et al. (2007) |
| IO + BrO → Br + I + 0.5$O_2$ | $3.0\times10^{-12}$ | -510 | Atkinson et al. (2007) |
| IO + BrO → Br + OIO | $1.2\times10^{-11}$ | -510 | Atkinson et al. (2007) |
| $CH_3I$ + OH → I + $H_2O$ + $HO_2$ | $2.9\times10^{-12}$ | 1100 | Sander et al. (2011b) |

Atmos. Chem. Phys. Discuss., https://doi.org/10.5194/acp-2017-903
Manuscript under review for journal Atmos. Chem. Phys.
Discussion started: 14 November 2017


Atmospheric Chemistry and Physics Discussions

**Table 3.** Termolecular reactions for halogens species included in WRF-Chem. The lower pressure limit rate ($K_0$) is given by $A_0 \times (\frac{T}{300})^a$. The high pressure limit ($K_\infty$) is given by $B_0 \times (\frac{300}{T})^b$. $F_c$ describes the fall of curve of the reaction described by Atkinson et al. (2007). Then the reaction rate (k) is defined as $K_0[M]/(1+\frac{K_0[M]}{K_\infty}) \times F_c^n$ and n as $(1+ (\log_{10} \frac{K_0[M]}{K_\infty})^2)^{-1}$.

| Termolecular reactions | $A_0$ | a | $B_0$ | b | $F_c$ | Reference |
|---|---|---|---|---|---|---|
| $Cl + NO_2 \xrightarrow{M} ClNO_2$ | $1.8\times10^{-31}$ | -2 | $1.0\times10^{-10}$ | -1 | 0.6 | Sander et al. (2011b) |
| $ClO + NO_2 \xrightarrow{M} ClNO_3$ | $1.8\times10^{-31}$ | -3.4 | $1.5\times10^{-11}$ | -1.9 | 0.4 | Sander et al. (2011b) |
| $Br + NO_2 \xrightarrow{M} BrNO_2$ | $4.2\times10^{-31}$ | -2.4 | $2.7\times10^{-11}$ | 0.0 | 0.55 | Sander et al. (2011b) |
| $BrO + NO_2 \xrightarrow{M} BrNO_3$ | $5.2\times10^{-31}$ | -3.2 | $6.9\times10^{-12}$ | -2.9 | 0.6 | Sander et al. (2011b) |
| $I + NO \xrightarrow{M} INO$ | $1.8\times10^{-32}$ | -1 | $1.7\times10^{-11}$ | 0.0 | 0.6 | Atkinson et al. (2007) |
| $I + NO_2 \xrightarrow{M} INO_2$ | $3.0\times10^{-31}$ | -1 | $6.6\times10^{-11}$ | 0.0 | 0.63 | Atkinson et al. (2007) |
| $IO + NO_2 \xrightarrow{M} INO_3$ | $7.7\times10^{-31}$ | -5 | $1.6\times10^{-11}$ | 0.0 | 0.4 | Atkinson et al. (2007) |

Atmos. Chem. Phys. Discuss., https://doi.org/10.5194/acp-2017-903
Manuscript under review for journal Atmos. Chem. Phys.
Discussion started: 14 November 2017


Atmospheric Chemistry and Physics Discussions

**Table 4.** Photolytic reactions of halogens included in WRF-Chem.

| Photolysis reactions |
|---|
| $Cl_2 \xrightarrow{h\nu} 2\ Cl$ |
| $OClO\ (+O_2) \xrightarrow{h\nu} O_3 + ClO$ |
| $HOCl \xrightarrow{h\nu} Cl + OH$ |
| $ClNO_2 \xrightarrow{h\nu} Cl + NO_2$ |
| $ClNO_3 \xrightarrow{h\nu} Cl + NO_3$ |
| $ClNO_3 \xrightarrow{h\nu} ClO + NO_2$ |
| $Br_2 \xrightarrow{h\nu} 2\ Br$ |
| $BrO \xrightarrow{h\nu} Br\ (+O_3)$ |
| $HOBr \xrightarrow{h\nu} Br + OH$ |
| $BrNO_2 \xrightarrow{h\nu} Br + NO_2$ |
| $BrNO_3 \xrightarrow{h\nu} Br + NO_3$ |
| $BrNO_3 \xrightarrow{h\nu} BrO + NO_2$ |
| $I_2 \xrightarrow{h\nu} 2\ I$ |
| $IO\ (+O_2) \xrightarrow{h\nu} I\ (+\ O_3)$ |
| $I_2O_4 \xrightarrow{h\nu} OIO + OIO$ |
| $OIO \xrightarrow{h\nu} I\ (+\ O2)$ |
| $I_2O_2 \xrightarrow{h\nu} I + OIO$ |
| $HOI \xrightarrow{h\nu} I + OH$ |
| $INO \xrightarrow{h\nu} I + NO$ |
| $INO_2 \xrightarrow{h\nu} I + NO_2$ |
| $INO_3 \xrightarrow{h\nu} I + NO_3$ |
| $I_2O_3 \xrightarrow{h\nu} OIO + IO$ |
| $IBr \xrightarrow{h\nu} I + Br$ |
| $ICl \xrightarrow{h\nu} I + Cl$ |
| $BrCl \xrightarrow{h\nu} Br + Cl$ |
| $CHBr_3\ (+O_2) \xrightarrow{h\nu} 3\ Br$ |
| $CH_3Br \xrightarrow{h\nu} Br + CH_3O_2$ |
| $CH_2Br_2 \xrightarrow{h\nu} 2Br$ |
| $CH_2BrCl \xrightarrow{h\nu} Br + Cl$ |
| $CHBrCl_2 \xrightarrow{h\nu} Br + 2\ Cl$ |
| $CHBr_2Cl \xrightarrow{h\nu} 2Br + Cl$ |
| $CH_2I_2 + (O_2) \xrightarrow{h\nu} 2\ I$ |
| $CH_3I \xrightarrow{h\nu} I + CH_3O_2$ |
| $CH_2ClI \xrightarrow{h\nu} I + Cl + 2\ HO_2 + CO$ |
| $CH_2IBr \xrightarrow{h\nu} Br + I$ |

Atmos. Chem. Phys. Discuss., https://doi.org/10.5194/acp-2017-903
Manuscript under review for journal Atmos. Chem. Phys.
Discussion started: 14 November 2017


Atmospheric Chemistry and Physics Discussions

**Table 5.** Halogen heterogeneous reactions implemented in WRF-Chem.

| Heterogeneous reactions | Note | Uptake coefficient |
|---|---|---|
| $INO_3 \rightarrow 0.5\ IBr + 0.5\ ICl + HNO_3$ | Sea salt only if pH < 5.5 | 0.01 |
| $INO_3 \rightarrow 0.5\ I_2 + HNO_3$ | Sea salt only if pH > 5.5 | 0.01 |
| $INO_2 \rightarrow 0.5\ IBr + 0.5\ ICl + HNO_3$ | Sea salt only if pH < 5.5 | 0.02 |
| $INO_2 \rightarrow 0.5\ I_2 + HNO_3$ | Sea salt only if pH > 5.5 | 0.02 |
| $HOI \rightarrow 0.5\ IBr + 0.5\ ICl$ | Sea salt only if pH < 5.5 | 0.06 |
| $HOI \rightarrow 0.5\ I_2$ | Sea salt only if pH > 5.5 | 0.06 |
| $BrNO_3 \rightarrow 0.6\ Br_2 + HNO_3$ | Sea salt only if pH < 5.5 | 0.08 |
| $BrNO_2 \rightarrow 0.6\ Br_2 + HNO_3$ | Sea salt only if pH < 5.5 | 0.04 |
| $HOBr \rightarrow 0.6\ Br_2$ | Sea salt only if pH < 5.5 | 0.1 |
| $I_2O_2 \rightarrow$ I(aerosol) | | 0.02 |
| $I_2O_3 \rightarrow$ I(aerosol) | | 0.02 |
| $I_2O_4 \rightarrow$ I(aerosol) | | 0.02 |
| $ClNO_3 \rightarrow HOCl + HNO_3$ | Hydrolysis | 0.001[a]/0.01[b] |
| $BrNO_3 \rightarrow HOBr + HNO_3$ | Hydrolysis | 0.03[a]/0.8[b] |
| $ClNO_3 + HCl \rightarrow Cl_2 + HNO_3$ | | 0.1 |
| $ClNO_3 + HBr \rightarrow BrCl + HNO_3$ | | 0.1 |
| $HOBr + HBr \rightarrow Br_2 + H_2O$ | | 0.1 |
| $HOBr + HCl \rightarrow BrCl + H_2O$ | | 0.1 |

[a] Uptake coefficient for moderate temperature

[b] Uptake coefficient for cold temperatures

Atmos. Chem. Phys. Discuss., https://doi.org/10.5194/acp-2017-903
Manuscript under review for journal Atmos. Chem. Phys.
Discussion started: 14 November 2017


Atmospheric Chemistry and Physics Discussions

**Table 6.** Model details and experiment configuration

| | |
|---|---|
| Chemistry | |
| Chemical mechanism | MOZART-4 (Emmons et al., 2010; Knote et al., 2014) |
| Halogen chemical mechanism | MISTRA (Sommariva and von Glasow, 2012) |
| Photolysis scheme | FTUV (Tie et al., 2003) |
| Dry deposition | Wesely (1989) |
| Wet deposition | Grell and Dévényi (2002) |
| Biogenic emissions | MEGAN (Guenther et al., 2006) |
| Halocarbons and OVOCs air-sea fluxes | Online calculation (Liss and Slater, 1974; Johnson, 2010) |
| Alkenes and alkanes oceanic emissions | POET (Granier et al., 2005) |
| Sea-salt emissions | $seas\_opt = 4$, Archer-Nicholls et al. (2014) |
| $N_2O_5$ heterogeneous chemistry | $n2o5\_hetchem = 2$, Lowe et al. (2015) |
| Resolution and Initial conditions | |
| Horizontal resolution | 30 km x 30 km |
| Vertical layers | 30 or 52 |
| Top of the atmosphere | 50 hPa |
| Chemical initial condition | GEOS-Chem (Sherwen et al., 2016b) |
| Meteorological initial condition | Era-Interim (Dee et al., 2011) |
| Chemistry spin-up | 20 days |

**Table 7.** Summary of all the simulations to investigate the main processes involving reactions between halogen chemistry.

| Simulation name | Oceanic fluxes | Debromination | Heterogeneous | Br-Alkenes | Br-Aldehydes | Halogens |
|---|---|---|---|---|---|---|
| WRF-DEBROM | Online | √ | √ | √ | √ | √ |
| WRF-ZIS | Prescribed | √ | √ | √ | √ | √ |
| WRF-NODEBROM | Online | | √ | √ | √ | √ |
| WRF-NOHET | Online | | | √ | √ | √ |
| WRF-NOALKE | Online | √ | √ | | √ | √ |
| WRF-NOALD | Online | √ | √ | √ | | √ |
| WRF-NOVOCS | Online | √ | √ | | | √ |
| WRF-NOHAL | - | | | | | |

Atmos. Chem. Phys. Discuss., https://doi.org/10.5194/acp-2017-903
Manuscript under review for journal Atmos. Chem. Phys.
Discussion started: 14 November 2017


Atmospheric Chemistry and Physics Discussions

**Table 8.** Integrated odd oxygen loss rates for each $O_3$ depleting halogen family within the troposphere at different altitude levels: MBL (surface - 900 hPa), FT (900 hPa- 350 hPa) and UT (350 hPa- Tropopause).

| Family | MBL | FT | UT | Troposphere |
|---|---|---|---|---|
| $BrO_x$ cycles (%) | 14.1 | 8.7 | 18.9 | 13.8 |
| $ClO_x$ cycles (%) | 0.9 | 0.6 | 0.6 | 0.7 |
| $IO_x$ cycles (%) | 18.8 | 9.0 | 20.6 | 16.0 |
| Halogen cycles (%) | 33.8 | 18.3 | 40.1 | 30.5 |



## References

S. J. Andrews, S. C. Hackenberg, and L. J. Carpenter. Technical Note: A fully automated purge and trap GC-MS system for quantification of volatile organic compound (VOC) fluxes between the ocean and atmosphere. *Ocean Science*, 11(2):313–321, 2015. doi:10.5194/os-11-313-2015. URL https://www.ocean-sci.net/11/313/2015/.

S. Archer-Nicholls, D. Lowe, S. Utembe, J. Allan, R. A. Zaveri, J. D. Fast, Ø. Hodnebrog, H. Denier van der Gon, and G. McFiggans. Gaseous chemistry and aerosol mechanism developments for version 3.5.1 of the online regional model, WRF-Chem. *Geoscientific Model Development*, 7(6):2557–2579, 2014. doi:10.5194/gmd-7-2557-2014. URL http://www.geosci-model-dev.net/7/2557/2014/.

R. Atkinson, D. L. Baulch, R. A. Cox, J. N. Crowley, R. F. Hampson, R. G. Hynes, M. E. Jenkin, M. J. Rossi, J. Troe, and I. Subcommittee. Evaluated kinetic and photochemical data for atmospheric chemistry: Volume II - gas phase reactions of organic species. *Atmospheric Chemistry and Physics*, 6(11):3625–4055, 2006. doi:10.5194/acp-6-3625-2006. URL http://www.atmos-chem-phys.net/6/3625/2006/.

R. Atkinson, D. L. Baulch, R. A. Cox, J. N. Crowley, R. F. Hampson, R. G. Hynes, M. E. Jenkin, M. J. Rossi, and J. Troe. Evaluated kinetic and photochemical data for atmospheric chemistry: Volume III - gas phase reactions of inorganic halogens. *Atmospheric Chemistry and Physics*, 7(4):981–1191, 2007. doi:10.5194/acp-7-981-2007. URL http://www.atmos-chem-phys.net/7/981/2007/.

R. Atkinson, D. L. Baulch, R. A. Cox, J. N. Crowley, R. F. Hampson, R. G. Hynes, M. E. Jenkin, M. J. Rossi, J. Troe, and T. J. Wallington. Evaluated kinetic and photochemical data for atmospheric chemistry: Volume IV - gas phase reactions of organic halogen species. *Atmospheric Chemistry and Physics*, 8(15):4141–4496, 2008. doi:10.5194/acp-8-4141-2008. URL http://www.atmos-chem-phys.net/8/4141/2008/.

E. Atlas, W. Pollock, J. Greenberg, L. Heidt, and A. M. Thompson. Alkyl nitrates, nonmethane hydrocarbons, and halocarbon gases over the equatorial Pacific Ocean during SAGA 3. *Journal of Geophysical Research: Atmospheres*, 98(D9):16933–16947, 1993. ISSN 2156-2202. doi:10.1029/93JD01005. URL http://dx.doi.org/10.1029/93JD01005.

N. Bell, L. Hsu, D. J. Jacob, M. G. Schultz, D. R. Blake, J. H. Butler, D. B. King, J. M. Lobert, and E. Maier-Reimer. Methyl iodide: Atmospheric budget and use as a tracer of marine convection in global models. *Journal of Geophysical Research: Atmospheres*, 107 (D17):ACH 8–1–ACH 8–12, 2002. ISSN 2156-2202. doi:10.1029/2001JD001151. URL http://dx.doi.org/10.1029/2001JD001151. 4340.

R. P. Bell. The Proton in Chemistry. *2nd Edn., Cornell University Press*, 1973.

W. J. Bloss, M. J. Evans, J. D. Lee, R. Sommariva, D. E. Heard, and M. J. Pilling. The oxidative capacity of the troposphere: Coupling of field measurements of oh and a global chemistry transport model. *Faraday Discuss.*, 130:425–436, 2005. doi:10.1039/B419090D. URL http://dx.doi.org/10.1039/B419090D.

B. Burkholder, S. P. Sander, J. Abbatt, J. R. Barker, R. E. Huie, C. E. Kolb, M. J. Kurylo, V. L. Orkin, D. M. Wilmouth, and W. P. H. Chemical kinetics and photochemical data for use in atmospheric studies, Evaluation number 18. Technical report, 2015.

L. J. Carpenter, S. M. MacDonald, M. D. Shaw, R. Kumar, R. W. Saunders, R. Parthipan, J. Wilson, and J. M. C. Plane. Atmospheric iodine levels influenced by sea surface emissions of inorganic iodine. *Nature Geosci*, 6(2):108–111, feb 2013. ISSN 1752-0894. doi:http://dx.doi.org/10.1038/ngeo1687. URL http://www.nature.com/ngeo/journal/v6/n2/abs/ngeo1687.html#supplementary-information. 10.1038/ngeo1687.

W. L. Chameides and D. D. Davis. Iodine: Its possible role in tropospheric photochemistry. *Journal of Geophysical Research: Oceans*, 85 (C12):7383–7398, 1980. ISSN 2156-2202. doi:10.1029/JC085iC12p07383. URL http://dx.doi.org/10.1029/JC085iC12p07383.

T. Class and K. Ballschmiter. Chemistry of organic traces in air. *Journal of Atmospheric Chemistry*, 6(1):35–46, 1988. ISSN 1573-0662. doi:10.1007/BF00048330. URL http://dx.doi.org/10.1007/BF00048330.

S. Coburn, I. Ortega, R. Thalman, B. Blomquist, C. W. Fairall, and R. Volkamer. Measurements of diurnal variations and eddy covariance (EC) fluxes of glyoxal in the tropical marine boundary layer: description of the Fast LED-CE-DOAS instrument. *Atmospheric Measurement Techniques*, 7(10):3579–3595, 2014. doi:10.5194/amt-7-3579-2014. URL http://www.atmos-meas-tech.net/7/3579/2014/.

D. P. Dee, S. M. Uppala, A. J. Simmons, P. Berrisford, P. Poli, S. Kobayashi, U. Andrae, M. A. Balmaseda, G. Balsamo, P. Bauer, P. Bechtold, A. C. M. Beljaars, L. van de Berg, J. Bidlot, N. Bormann, C. Delsol, R. Dragani, M. Fuentes, A. J. Geer, L. Haimberger, S. B. Healy, H. Hersbach, E. V. Hólm, L. Isaksen, P. Kållberg, M. Köhler, M. Matricardi, A. P. McNally, B. M. Monge-Sanz, J.-J. Morcrette, B.-K. Park, C. Peubey, P. de Rosnay, C. Tavolato, J.-N. Thépaut, and F. Vitart. The ERA-Interim reanalysis: configuration and performance of the data assimilation system. *Quarterly Journal of the Royal Meteorological Society*, 137(656):553–597, 2011. ISSN 1477-870X. doi:10.1002/qj.828. URL http://dx.doi.org/10.1002/qj.828.

B. Dix, S. Baidar, J. F. Bresch, S. R. Hall, K. S. Schmidt, S. Wang, and R. Volkamer. Detection of iodine monoxide in the tropical free troposphere. *Proceedings of the National Academy of Sciences of the United States of America*, 110(6):2035–2040, jan 2013. ISSN 0027-8424 1091-6490. URL http://www.ncbi.nlm.nih.gov/pmc/articles/PMC3568334/.

B. Dix, T. K. Koenig, and R. Volkamer. Parameterization retrieval of trace gas volume mixing ratios from Airborne MAX-DOAS. *Atmospheric Measurement Techniques*, 9(11):5655–5675, 2016. doi:10.5194/amt-9-5655-2016. URL https://www.atmos-meas-tech.net/9/5655/2016/.

L. K. Emmons, S. Walters, P. G. Hess, J.-F. Lamarque, G. G. Pfister, D. Fillmore, C. Granier, A. Guenther, D. Kinnison, T. Laepple, J. Orlando, X. Tie, G. Tyndall, C. Wiedinmyer, S. L. Baughcum, and S. Kloster. Description and evaluation of the Model for Ozone and Related chemical Tracers, version 4 (MOZART-4). *Geoscientific Model Development*, 3(1):43–67, 2010. doi:10.5194/gmd-3-43-2010.

R. P. Fernandez, R. J. Salawitch, D. E. Kinnison, J.-F. Lamarque, and A. Saiz-Lopez. Bromine partitioning in the tropical tropopause layer: implications for stratospheric injection. *Atmospheric Chemistry and Physics*, 14(24):13391–13410, 2014. doi:10.5194/acp-14-13391-2014. URL http://www.atmos-chem-phys.net/14/13391/2014/.

A. Frenzel, V. Scheer, R. Sikorski, C. George, W. Behnke, and C. Zetzsch. Heterogeneous Interconversion Reactions of $BrNO_2$, $ClNO_2$, $Br_2$, and $Cl_2$. *The Journal of Physical Chemistry A*, 102(8):1329–1337, 1998. doi:10.1021/jp973044b. URL http://dx.doi.org/10.1021/jp973044b.

B. Gantt, G. Sarwar, J. Xing, H. Simon, D. Schwede, W. T. Hutzell, R. Mathur, and A. Saiz-Lopez. The Impact of Iodide-Mediated Ozone Deposition and Halogen Chemistry on Surface Ozone Concentrations Across the Continental United States. *Environmental Science & Technology*, 51(3):1458–1466, 2017. doi:10.1021/acs.est.6b03556. URL http://dx.doi.org/10.1021/acs.est.6b03556. PMID: 28051851.

J. C. Gómez Martín, P. Spietz, and J. P. Burrows. Spectroscopic studies of the $I_2/O_3$ photochemistry: Part 1: Determination of the absolute absorption cross sections of iodine oxides of atmospheric relevance . *Journal of Photochemistry and Photobiology A: Chemistry*, 176 (1–3):15 – 38, 2005. ISSN 1010-6030. doi:http://dx.doi.org/10.1016/j.jphotochem.2005.09.024. URL http://www.sciencedirect.com/science/article/pii/S1010603005004661. In Honour of Professor Richard P. Wayne.

J. C. Gómez Martín, P. Spietz, and J. P. Burrows. Kinetic and Mechanistic Studies of the $I_2/O_3$ Photochemistry. *The Journal of Physical Chemistry A*, 111(2):306–320, 2007. doi:10.1021/jp061186c. URL http://dx.doi.org/10.1021/jp061186c. PMID: 17214469.

C. Granier, J. Lamarque, A. Mieville, J. Muller, J. Olivier, J. Orlando, J. Peters, G. Petron, G. Tyndall, and S. Wallens. POET, a database of surface emissions of ozone precursors. *http://www. aero. jussieu. fr/projet/ACCENT/POET. php*, 6988(6989):30, 2005.

G. A. Grell and D. o. Dévényi. A generalized approach to parameterizing convection combining ensemble and data assimilation techniques. *Geophysical Research Letters*, 29(14):38–1–38–4, 2002. ISSN 1944-8007. doi:10.1029/2002GL015311. URL http://dx.doi.org/10.1029/2002GL015311.

G. A. Grell, S. E. Peckham, R. Schmitz, S. A. McKeen, G. Frost, W. C. Skamarock, and B. Eder. Fully coupled "online"chemistry within the WRF model. *Atmospheric Environment*, 39(37):6957 – 6975, 2005. ISSN 1352-2310. doi:http://dx.doi.org/10.1016/j.atmosenv.2005.04.027. URL http://www.sciencedirect.com/science/article/pii/S1352231005003560.

A. Guenther, T. Karl, P. Harley, C. Wiedinmyer, P. I. Palmer, and C. Geron. Estimates of global terrestrial isoprene emissions using MEGAN (Model of Emissions of Gases and Aerosols from Nature). *Atmospheric Chemistry and Physics*, 6(11):3181–3210, 2006. doi:10.5194/acp-6-3181-2006.

J. C. Gómez Martín, A. S. Mahajan, T. D. Hay, C. Prados-Román, C. Ordóñez, S. M. MacDonald, J. M. Plane, M. Sorribas, M. Gil, J. F. Paredes Mora, M. V. Agama Reyes, D. E. Oram, E. Leedham, and A. Saiz-Lopez. Iodine chemistry in the eastern Pacific marine boundary layer. *Journal of Geophysical Research: Atmospheres*, 118(2):887–904, 2013. ISSN 2169-8996. doi:10.1002/jgrd.50132. URL http://dx.doi.org/10.1002/jgrd.50132.

N. R. P. Harris, L. J. Carpenter, J. D. Lee, G. Vaughan, M. T. Filus, R. L. Jones, B. OuYang, J. A. Pyle, A. D. Robinson, S. J. Andrews, A. C. Lewis, J. Minaeian, A. Vaughan, J. R. Dorsey, M. W. Gallagher, M. L. Breton, R. Newton, C. J. Percival, H. M. A. Ricketts, S. J.-B. Bauguitte, G. J. Nott, A. Wellpott, M. J. Ashfold, J. Flemming, R. Butler, P. I. Palmer, P. H. Kaye, C. Stopford, C. Chemel, H. Boesch, N. Humpage, A. Vick, A. R. MacKenzie, R. Hyde, P. Angelov, E. Meneguz, and A. J. Manning. Coordinated Airborne Studies in the Tropics (CAST). *Bulletin of the American Meteorological Society*, 98(1):145–162, 2017. doi:10.1175/BAMS-D-14-00290.1. URL https://doi.org/10.1175/BAMS-D-14-00290.1.

R. Hossaini, M. P. Chipperfield, B. M. Monge-Sanz, N. A. D. Richards, E. Atlas, and D. R. Blake. Bromoform and dibromomethane in the tropics: a 3-D model study of chemistry and transport. *Atmospheric Chemistry and Physics*, 10(2):719–735, 2010. doi:10.5194/acp-10-719-2010. URL https://www.atmos-chem-phys.net/10/719/2010/.

R. Hossaini, H. Mantle, M. P. Chipperfield, S. A. Montzka, P. Hamer, F. Ziska, B. Quack, K. Krüger, S. Tegtmeier, E. Atlas, S. Sala, A. Engel, H. Bönisch, T. Keber, D. Oram, G. Mills, C. Ordóñez, A. Saiz-Lopez, N. Warwick, Q. Liang, W. Feng, F. Moore, B. R. Miller, V. Marécal, N. A. D. Richards, M. Dorf, and K. Pfeilsticker. Evaluating global emission inventories of biogenic bromocarbons. *Atmospheric Chemistry and Physics*, 13(23):11819–11838, 2013. doi:10.5194/acp-13-11819-2013. URL http://www.atmos-chem-phys.net/13/11819/2013/.

R. Hossaini, P. K. Patra, A. A. Leeson, G. Krysztofiak, N. L. Abraham, S. J. Andrews, A. T. Archibald, J. Aschmann, E. L. Atlas, D. A. Belikov, H. Bönisch, L. J. Carpenter, S. Dhomse, M. Dorf, A. Engel, W. Feng, S. Fuhlbrügge, P. T. Griffiths, N. R. P. Harris, R. Hommel, T. Keber, K. Krüger, S. T. Lennartz, S. Maksyutov, H. Mantle, G. P. Mills, B. Miller, S. A. Montzka, F. Moore, M. A. Navarro, D. E. Oram, K. Pfeilsticker, J. A. Pyle, B. Quack, A. D. Robinson, E. Saikawa, A. Saiz-Lopez, S. Sala, B.-M. Sinnhuber, S. Taguchi, S. Tegtmeier, R. T. Lidster, C. Wilson, and F. Ziska. A multi-model intercomparison of halogenated very short-lived substances (TransCom-VSLS): linking oceanic emissions and tropospheric transport for a reconciled estimate of the stratospheric source gas injection of bromine. *Atmospheric Chemistry and Physics*, 16(14):9163–9187, 2016. doi:10.5194/acp-16-9163-2016. URL http://www.atmos-chem-phys.net/16/9163/2016/.

D. J. Jacob. Heterogeneous chemistry and tropospheric ozone, atmos. *Environ*, 34:2131–2159, 2000.

E. J. Jensen, L. Pfister, D. E. Jordan, T. V. Bui, R. Ueyama, H. B. Singh, T. D. Thornberry, A. W. Rollins, R.-S. Gao, D. W. Fahey, K. H. Rosenlof, J. W. Elkins, G. S. Diskin, J. P. DiGangi, R. P. Lawson, S. Woods, E. L. Atlas, M. A. N. Rodriguez, S. C. Wofsy, J. Pittman, C. G. Bardeen, O. B. Toon, B. C. Kindel, P. A. Newman, M. J. McGill, D. L. Hlavka, L. R. Lait, M. R. Schoeberl, J. W. Bergman, H. B. Selkirk, M. J. Alexander, J.-E. Kim, B. H. Lim, J. Stutz, and K. Pfeilsticker. The NASA Airborne Tropical Tropopause Experiment: High-Altitude Aircraft Measurements in the Tropical Western Pacific. *Bulletin of the American Meteorological Society*, 98(1):129–143, 2017. doi:10.1175/BAMS-D-14-00263.1. URL https://doi.org/10.1175/BAMS-D-14-00263.1.

M. T. Johnson. A numerical scheme to calculate temperature and salinity dependent air-water transfer velocities for any gas. *Ocean Science*, 6(4):913–932, 2010. doi:10.5194/os-6-913-2010. URL http://www.ocean-sci.net/6/913/2010/.

W. C. Keene, R. Sander, A. A. Pszenny, R. Vogt, P. J. Crutzen, and J. N. Galloway. Aerosol pH in the marine boundary layer: A review and model evaluation . *Journal of Aerosol Science*, 29(3):339 – 356, 1998. ISSN 0021-8502. doi:http://dx.doi.org/10.1016/S0021-8502(97)10011-8. URL http://www.sciencedirect.com/science/article/pii/S0021850297100118.

C. Knote, A. Hodzic, J. L. Jimenez, R. Volkamer, J. J. Orlando, S. Baidar, J. Brioude, J. Fast, D. R. Gentner, A. H. Goldstein, P. L. Hayes, W. B. Knighton, H. Oetjen, A. Setyan, H. Stark, R. Thalman, G. Tyndall, R. Washenfelder, E. Waxman, and Q. Zhang. Simulation of semi-explicit mechanisms of SOA formation from glyoxal in aerosol in a 3-D model. *Atmospheric Chemistry and Physics*, 14(12):6213–6239, 2014. doi:10.5194/acp-14-6213-2014. URL http://www.atmos-chem-phys.net/14/6213/2014/.

T. K. Koenig, R. Volkamer, S. Baidar, B. Dix, S. Wang, D. C. Anderson, R. J. Salawitch, P. A. Wales, C. A. Cuevas, R. P. Fernandez, A. Saiz-Lopez, M. J. Evans, T. Sherwen, D. J. Jacob, J. Schmidt, D. Kinnison, J.-F. Lamarque, E. C. Apel, J. C. Bresch, T. Campos, F. M. Flocke, S. R. Hall, S. B. Honomichl, R. Hornbrook, J. B. Jensen, R. Lueb, D. D. Montzka, L. L. Pan, J. M. Reeves, S. M. Schauffler, K. Ullmann, A. J. Weinheimer, E. L. Atlas, V. Donets, M. A. Navarro, D. Riemer, N. J. Blake, D. Chen, L. G. Huey, D. J. Tanner, T. F. Hanisco, and G. M. Wolfe. BrO and $Br_y$ profiles over the Western Pacific: Relevance of Inorganic Bromine Sources and a $Br_y$ Minimum in the Aged Tropical Tropopause Layer. *Atmospheric Chemistry and Physics Discussions*, 2017:1–46, 2017. doi:10.5194/acp-2017-572. URL https://www.atmos-chem-phys-discuss.net/acp-2017-572/.

S. J. Lawson, P. W. Selleck, I. E. Galbally, M. D. Keywood, M. J. Harvey, C. Lerot, D. Helmig, and Z. Ristovski. Seasonal in situ observations of glyoxal and methylglyoxal over the temperate oceans of the Southern Hemisphere. *Atmospheric Chemistry and Physics*, 15(1):223–240, 2015. doi:10.5194/acp-15-223-2015. URL http://www.atmos-chem-phys.net/15/223/2015/.

S. T. Lennartz, G. Krysztofiak, C. A. Marandino, B.-M. Sinnhuber, S. Tegtmeier, F. Ziska, R. Hossaini, K. Krüger, S. A. Montzka, E. Atlas, D. E. Oram, T. Keber, H. Bönisch, and B. Quack. Modelling marine emissions and atmospheric distributions of halocarbons and dimethyl sulfide: the influence of prescribed water concentration vs. prescribed emissions. *Atmospheric Chemistry and Physics*, 15(20):11753–11772, 2015. doi:10.5194/acp-15-11753-2015. URL http://www.atmos-chem-phys.net/15/11753/2015/.

Q. Li, L. Zhang, T. Wang, Y. J. Tham, R. Ahmadov, L. Xue, Q. Zhang, and J. Zheng. Impacts of heterogeneous uptake of dinitrogen pentoxide and chlorine activation on ozone and reactive nitrogen partitioning: improvement and application of the WRF-Chem model in southern China. *Atmospheric Chemistry and Physics*, 16(23):14875–14890, 2016. doi:10.5194/acp-16-14875-2016. URL http://www.atmos-chem-phys.net/16/14875/2016/.

P. S. Liss and P. G. Slater. Flux of Gases across the Air-Sea Interface. *Nature*, 247(5438):181–184, jan 1974. doi:http://dx.doi.org/10.1038/247181a0. 10.1038/247181a0.

M. S. Long, W. C. Keene, R. C. Easter, R. Sander, X. Liu, A. Kerkweg, and D. Erickson. Sensitivity of tropospheric chemical composition to halogen-radical chemistry using a fully coupled size-resolved multiphase chemistry-global climate system: halogen distributions, aerosol composition, and sensitivity of climate-relevant gases. *Atmospheric Chemistry and Physics*, 14(7):3397–3425, 2014. doi:10.5194/acp-14-3397-2014. URL http://www.atmos-chem-phys.net/14/3397/2014/.

D. Lowe, D. Topping, and G. McFiggans. Modelling multi-phase halogen chemistry in the remote marine boundary layer: investigation of the influence of aerosol size resolution on predicted gas- and condensed-phase chemistry. *Atmospheric Chemistry and Physics*, 9(14):4559–4573, 2009. doi:10.5194/acp-9-4559-2009. URL http://www.atmos-chem-phys.net/9/4559/2009/.

D. Lowe, S. Archer-Nicholls, W. Morgan, J. Allan, S. Utembe, B. Ouyang, E. Aruffo, M. Le Breton, R. A. Zaveri, P. Di Carlo, C. Percival, H. Coe, R. Jones, and G. McFiggans. WRF-Chem model predictions of the regional impacts of $N_2O_5$ heterogeneous processes on night-

time chemistry over north-western Europe. *Atmospheric Chemistry and Physics*, 15(3):1385–1409, 2015. doi:10.5194/acp-15-1385-2015. URL http://www.atmos-chem-phys.net/15/1385/2015/.

S. M. MacDonald, J. C. Gómez Martín, R. Chance, S. Warriner, A. Saiz-Lopez, L. J. Carpenter, and J. M. C. Plane. A laboratory characterisation of inorganic iodine emissions from the sea surface: dependence on oceanic variables and parameterisation for global modelling. *Atmospheric Chemistry and Physics*, 14(11):5841–5852, 2014. doi:10.5194/acp-14-5841-2014. URL http://www.atmos-chem-phys.net/14/5841/2014/.

A. S. Mahajan, J. C. Gómez Martín, T. D. Hay, S.-J. Royer, S. Yvon-Lewis, Y. Liu, L. Hu, C. Prados-Roman, C. Ordóñez, J. M. C. Plane, and A. Saiz-Lopez. Latitudinal distribution of reactive iodine in the Eastern Pacific and its link to open ocean sources. *Atmospheric Chemistry and Physics*, 12(23):11609–11617, 2012. doi:10.5194/acp-12-11609-2012. URL https://www.atmos-chem-phys.net/12/11609/2012/.

A. S. Mahajan, C. Prados-Roman, T. D. Hay, J. Lampel, D. Pöhler, K. Gro$\beta$mann, J. Tschritter, U. Frieß, U. Platt, P. Johnston, K. Kreher, F. Wittrock, J. P. Burrows, J. M. Plane, and A. Saiz-Lopez. Glyoxal observations in the global marine boundary layer. *Journal of Geophysical Research: Atmospheres*, 119(10):6160–6169, 2014. ISSN 2169-8996. doi:10.1002/2013JD021388. URL http://dx.doi.org/10.1002/2013JD021388. 2013JD021388.

G. McFiggans, J. M. C. Plane, B. J. Allan, L. J. Carpenter, H. Coe, and C. O'Dowd. A modeling study of iodine chemistry in the marine boundary layer. *Journal of Geophysical Research: Atmospheres*, 105(D11):14371–14385, 2000. ISSN 2156-2202. doi:10.1029/1999JD901187. URL http://dx.doi.org/10.1029/1999JD901187.

D. B. Millet, A. Guenther, D. A. Siegel, N. B. Nelson, H. B. Singh, J. A. de Gouw, C. Warneke, J. Williams, G. Eerdekens, V. Sinha, T. Karl, F. Flocke, E. Apel, D. D. Riemer, P. I. Palmer, and M. Barkley. Global atmospheric budget of acetaldehyde: 3-D model analysis and constraints from in-situ and satellite observations. *Atmospheric Chemistry and Physics*, 10(7):3405–3425, 2010. doi:10.5194/acp-10-3405-2010. URL http://www.atmos-chem-phys.net/10/3405/2010/.

M. Muñiz-Unamunzaga, R. Borge, G. Sarwar, B. Gantt, D. de la Paz, C. A. Cuevas, and A. Saiz-Lopez. The influence of ocean halogen and sulfur emissions in the air quality of a coastal megacity: The case of Los Angeles. *Science of The Total Environment*, 2017. ISSN 0048-9697. doi:http://dx.doi.org/10.1016/j.scitotenv.2017.06.098. URL http://www.sciencedirect.com/science/article/pii/S0048969717315024.

S. Myriokefalitakis, M. Vrekoussis, K. Tsigaridis, F. Wittrock, A. Richter, C. Brühl, R. Volkamer, J. P. Burrows, and M. Kanakidou. The influence of natural and anthropogenic secondary sources on the glyoxal global distribution. *Atmospheric Chemistry and Physics*, 8(16):4965–4981, 2008. doi:10.5194/acp-8-4965-2008. URL http://www.atmos-chem-phys.net/8/4965/2008/.

C. Ordóñez, J.-F. Lamarque, S. Tilmes, D. E. Kinnison, E. L. Atlas, D. R. Blake, G. Sousa Santos, G. Brasseur, and A. Saiz-Lopez. Bromine and iodine chemistry in a global chemistry-climate model: description and evaluation of very short-lived oceanic sources. *Atmospheric Chemistry and Physics*, 12(3):1423–1447, 2012. doi:10.5194/acp-12-1423-2012. URL http://www.atmos-chem-phys.net/12/1423/2012/.

J. J. Orlando and G. S. Tyndall. Rate Coefficients for the Thermal Decomposition of $BrONO_2$ and the Heat of Formation of $BrONO_2$. *The Journal of Physical Chemistry*, 100(50):19398–19405, 1996. doi:10.1021/jp9620274.

L. L. Pan, E. L. Atlas, R. J. Salawitch, S. B. Honomichl, J. F. Bresch, W. J. Randel, E. C. Apel, R. S. Hornbrook, A. J. Weinheimer, D. C. Anderson, S. J. Andrews, S. Baidar, S. P. Beaton, T. L. Campos, L. J. Carpenter, D. Chen, B. Dix, V. Donets, S. R. Hall, T. F. Hanisco, C. R. Homeyer, L. G. Huey, J. B. Jensen, L. Kaser, D. E. Kinnison, T. K. Koenig, J.-F. Lamarque, C. Liu, J. Luo, Z. J. Luo, D. D. Montzka, J. M. Nicely, R. B. Pierce, D. D. Riemer, T. Robinson, P. Romashkin, A. Saiz-Lopez, S. Schauffler, O. Shieh, M. H. Stell, K. Ullmann, G. Vaughan, R. Volkamer, and G. Wolfe. The Convective Transport of Active Species in the Tropics (CONTRAST) Experiment. *Bulletin of the American Meteorological Society*, 98(1):106–128, 2017. doi:10.1175/BAMS-D-14-00272.1. URL https://doi.org/10.1175/BAMS-D-14-00272.1.

J. P. Parrella, D. J. Jacob, Q. Liang, Y. Zhang, L. J. Mickley, B. Miller, M. J. Evans, X. Yang, J. A. Pyle, N. Theys, and M. Van Roozendael. Tropospheric bromine chemistry: implications for present and pre-industrial ozone and mercury. *Atmospheric Chemistry and Physics*, 12 (15):6723–6740, 2012. doi:10.5194/acp-12-6723-2012. URL http://www.atmos-chem-phys.net/12/6723/2012/.

C. Prados-Roman, C. A. Cuevas, R. P. Fernandez, D. E. Kinnison, J.-F. Lamarque, and A. Saiz-Lopez. A negative feedback between anthropogenic ozone pollution and enhanced ocean emissions of iodine. *Atmospheric Chemistry and Physics*, 15(4):2215–2224, 2015. doi:10.5194/acp-15-2215-2015. URL https://www.atmos-chem-phys.net/15/2215/2015/.

A. Saiz-Lopez and R. von Glasow. Reactive halogen chemistry in the troposphere. *Chem. Soc. Rev.*, 41:6448–6472, 2012. doi:10.1039/C2CS35208G. URL http://dx.doi.org/10.1039/C2CS35208G.

A. Saiz-Lopez, J. M. C. Plane, G. McFiggans, P. I. Williams, S. M. Ball, M. Bitter, R. L. Jones, C. Hongwei, and T. Hoffmann. Modelling molecular iodine emissions in a coastal marine environment: the link to new particle formation. *Atmospheric Chemistry and Physics*, 6 (4):883–895, 2006. doi:10.5194/acp-6-883-2006. URL https://www.atmos-chem-phys.net/6/883/2006/.

A. Saiz-Lopez, J.-F. Lamarque, D. E. Kinnison, S. Tilmes, C. Ordóñez, J. J. Orlando, A. J. Conley, J. M. C. Plane, A. S. Mahajan, G. Sousa Santos, E. L. Atlas, D. R. Blake, S. P. Sander, S. Schauffler, A. M. Thompson, and G. Brasseur. Estimating the climate significance of halogen-driven ozone loss in the tropical marine troposphere. *Atmospheric Chemistry and Physics*, 12(9):3939–3949, 2012a. doi:10.5194/acp-12-3939-2012. URL https://www.atmos-chem-phys.net/12/3939/2012/.

A. Saiz-Lopez, J. M. C. Plane, A. R. Baker, L. J. Carpenter, R. von Glasow, J. C. Gómez Martín, G. McFiggans, and R. W. Saunders. Atmospheric chemistry of iodine. *Chemical Reviews*, 112(3):1773–1804, 2012b. doi:10.1021/cr200029u. URL http://dx.doi.org/10.1021/cr200029u. PMID: 22032347.

A. Saiz-Lopez, R. P. Fernandez, C. Ordóñez, D. E. Kinnison, J. C. Gómez Martín, J.-F. Lamarque, and S. Tilmes. Iodine chemistry in the troposphere and its effect on ozone. *Atmospheric Chemistry and Physics*, 14(23):13119–13143, 2014. doi:10.5194/acp-14-13119-2014. URL http://www.atmos-chem-phys.net/14/13119/2014/.

A. Saiz-Lopez, S. Baidar, C. A. Cuevas, T. K. Koenig, R. P. Fernandez, B. Dix, D. E. Kinnison, J.-F. Lamarque, X. Rodriguez-Lloveras, T. L. Campos, and R. Volkamer. Injection of iodine to the stratosphere. *Geophysical Research Letters*, 42(16):6852–6859, 2015. ISSN 1944-8007. doi:10.1002/2015GL064796. URL http://dx.doi.org/10.1002/2015GL064796. 2015GL064796.

R. Sander. Compilation of Henry's law constants (version 4.0) for water as solvent. *Atmospheric Chemistry and Physics*, 15(8):4399–4981, 2015. doi:10.5194/acp-15-4399-2015. URL http://www.atmos-chem-phys.net/15/4399/2015/.

R. Sander and P. J. Crutzen. Model study indicating halogen activation and ozone destruction in polluted air masses transported to the sea. *Journal of Geophysical Research: Atmospheres*, 101(D4):9121–9138, 1996. ISSN 2156-2202. doi:10.1029/95JD03793. URL http://dx.doi.org/10.1029/95JD03793.

R. Sander, A. Baumgaertner, S. Gromov, H. Harder, P. Jöckel, A. Kerkweg, D. Kubistin, E. Regelin, H. Riede, A. Sandu, D. Taraborrelli, H. Tost, and Z.-Q. Xie. The atmospheric chemistry box model CAABA/MECCA-3.0. *Geoscientific Model Development*, 4(2):373–380, 2011a. doi:10.5194/gmd-4-373-2011. URL http://www.geosci-model-dev.net/4/373/2011/.

S. P. Sander, D. M. Golden, M. J. Kurylo, G. K. Moortgat, P. H. Wine, A. R. Ravishankara, C. E. Kolb, M. J. Molina, B. J. Finlayson-Pitts, R. E. Huie, and V. L. Orkin. Chemical kinetics and photochemical data for use in atmospheric studies, Evaluation number 15. Technical report, 2006.

S. P. Sander, R. R. Friedl, J. P. D. Abbatt, J. R. Barker, J. B. Burkholder, D. M. Golden, C. E. Kolb, M. J. Kurylo, G. K. Moortgat, P. H. Wine, R. E. Huie, and V. L. Orkin. Chemical kinetics and photochemical data for use in atmospheric studies, Evaluation Number 17,. Technical report, 2011b.

G. Sarwar, H. Simon, J. Xing, and R. Mathur. Importance of tropospheric $ClNO_2$ chemistry across the Northern Hemisphere. *Geophysical Research Letters*, 41(11):4050–4058, 2014. ISSN 1944-8007. doi:10.1002/2014GL059962. URL http://dx.doi.org/10.1002/2014GL059962. 2014GL059962.

G. Sarwar, B. Gantt, D. Schwede, K. Foley, R. Mathur, and A. Saiz-Lopez. Impact of Enhanced Ozone Deposition and Halogen Chemistry on Tropospheric Ozone over the Northern Hemisphere. *Environmental Science & Technology*, 49(15):9203–9211, 2015. doi:10.1021/acs.est.5b01657. URL http://dx.doi.org/10.1021/acs.est.5b01657. PMID: 26151227.

J. A. Schmidt, D. J. Jacob, H. M. Horowitz, L. Hu, T. Sherwen, M. J. Evans, Q. Liang, R. M. Suleiman, D. E. Oram, M. Le Breton, C. J. Percival, S. Wang, B. Dix, and R. Volkamer. Modeling the observed tropospheric BrO background: Importance of multiphase chemistry and implications for ozone, OH, and mercury. *Journal of Geophysical Research: Atmospheres*, 121(19):11,819–11,835, 2016. ISSN 2169-8996. doi:10.1002/2015JD024229. URL http://dx.doi.org/10.1002/2015JD024229. 2015JD024229.

F. Schweitzer, P. Mirabel, and C. George. Uptake of Hydrogen Halides by Water Droplets. *The Journal of Physical Chemistry A*, 104(1): 72–76, 2000. doi:10.1021/jp992621o. URL http://dx.doi.org/10.1021/jp992621o.

T. Sherwen, M. J. Evans, L. J. Carpenter, S. J. Andrews, R. T. Lidster, B. Dix, T. K. Koenig, R. Sinreich, I. Ortega, R. Volkamer, A. Saiz-Lopez, C. Prados-Roman, A. S. Mahajan, and C. Ordóñez. Iodine's impact on tropospheric oxidants: a global model study in GEOS-Chem. *Atmospheric Chemistry and Physics*, 16(2):1161–1186, 2016a. doi:10.5194/acp-16-1161-2016. URL http://www.atmos-chem-phys.net/16/1161/2016/.

T. Sherwen, J. A. Schmidt, M. J. Evans, L. J. Carpenter, K. Großmann, S. D. Eastham, D. J. Jacob, B. Dix, T. K. Koenig, R. Sinreich, I. Ortega, R. Volkamer, A. Saiz-Lopez, C. Prados-Roman, A. S. Mahajan, and C. Ordóñez. Global impacts of tropospheric halogens (Cl, Br, I) on oxidants and composition in GEOS-Chem. *Atmospheric Chemistry and Physics*, 16(18):12239–12271, 2016b. doi:10.5194/acp-16-12239-2016. URL http://www.atmos-chem-phys.net/16/12239/2016/.

W. R. Simpson, S. S. Brown, A. Saiz-Lopez, J. A. Thornton, and R. v. Glasow. Tropospheric Halogen Chemistry: Sources, Cycling, and Impacts. *Chemical Reviews*, 115(10):4035–4062, 2015. doi:10.1021/cr5006638. URL http://dx.doi.org/10.1021/cr5006638. PMID: 25763598.

R. Sinreich, S. Coburn, B. Dix, and R. Volkamer. Ship-based detection of glyoxal over the remote tropical Pacific Ocean. *Atmospheric Chemistry and Physics*, 10(23):11359–11371, 2010. doi:10.5194/acp-10-11359-2010. URL https://www.atmos-chem-phys.net/10/11359/2010/.

R. Sommariva and R. von Glasow. Multiphase Halogen Chemistry in the Tropical Atlantic Ocean. *Environmental Science & Technology*, 46 (19):10429–10437, 2012. doi:10.1021/es300209f. PMID: 22655856.

R. Sommariva, W. Bloss, and R. von Glasow. Uncertainties in gas-phase atmospheric iodine chemistry. *Atmospheric Environment*, 57:219 – 232, 2012. ISSN 1352-2310. doi:http://dx.doi.org/10.1016/j.atmosenv.2012.04.032. URL http://www.sciencedirect.com/science/article/pii/S1352231012003627.

X. Tie, S. Madronich, S. Walters, R. Zhang, P. Rasch, and W. Collins. Effect of clouds on photolysis and oxidants in the troposphere. *Journal of Geophysical Research: Atmospheres*, 108(D20):n/a–n/a, 2003. ISSN 2156-2202. doi:10.1029/2003JD003659. URL http://dx.doi.org/10.1029/2003JD003659. 4642.

K. Toyota, Y. Kanaya, M. Takahashi, and H. Akimoto. A box model study on photochemical interactions between VOCs and reactive halogen species in the marine boundary layer. *Atmospheric Chemistry and Physics*, 4(7):1961–1987, 2004. doi:10.5194/acp-4-1961-2004. URL http://www.atmos-chem-phys.net/4/1961/2004/.

R. Volkamer, S. Baidar, T. L. Campos, S. Coburn, J. P. DiGangi, B. Dix, E. W. Eloranta, T. K. Koenig, B. Morley, I. Ortega, B. R. Pierce, M. Reeves, R. Sinreich, S. Wang, M. A. Zondlo, and P. A. Romashkin. Aircraft measurements of BrO, IO, glyoxal, $NO_2$, $H_2O$, $O_2$–$O_2$ and aerosol extinction profiles in the tropics: comparison with aircraft-/ship-based in situ and lidar measurements. *Atmospheric Measurement Techniques*, 8(5):2121–2148, 2015. doi:10.5194/amt-8-2121-2015. URL http://www.atmos-meas-tech.net/8/2121/2015/.

R. von Glasow, R. Sander, A. Bott, and P. J. Crutzen. Modeling halogen chemistry in the marine boundary layer 1. Cloud-free MBL. *Journal of Geophysical Research: Atmospheres*, 107(D17):ACH 9–1–ACH 9–16, 2002a. ISSN 2156-2202. doi:10.1029/2001JD000942. URL http://dx.doi.org/10.1029/2001JD000942. 4341.

R. von Glasow, R. Sander, A. Bott, and P. J. Crutzen. Modeling halogen chemistry in the marine boundary layer. 1. Cloud-free MBL. *J. Geophys. Res.*, 107:4341, 2002b.

R. von Glasow, R. von Kuhlmann, M. G. Lawrence, U. Platt, and P. J. Crutzen. Impact of reactive bromine chemistry in the troposphere. *Atmospheric Chemistry and Physics*, 4(11/12):2481–2497, 2004. doi:10.5194/acp-4-2481-2004. URL http://www.atmos-chem-phys.net/4/2481/2004/.

S. Wang, J. A. Schmidt, S. Baidar, S. Coburn, B. Dix, T. K. Koenig, E. Apel, D. Bowdalo, T. L. Campos, E. Eloranta, M. J. Evans, J. P. DiGangi, M. A. Zondlo, R.-S. Gao, J. A. Haggerty, S. R. Hall, R. S. Hornbrook, D. Jacob, B. Morley, B. Pierce, M. Reeves, P. Romashkin, A. ter Schure, and R. Volkamer. Active and widespread halogen chemistry in the tropical and subtropical free troposphere. *Proceedings of the National Academy of Sciences*, 112(30):9281–9286, 2015. doi:10.1073/pnas.1505142112. URL http://www.pnas.org/content/112/30/9281.abstract.

M. Wesely. Parameterization of surface resistances to gaseous dry deposition in regional-scale numerical models . *Atmospheric Environment (1967)*, 23(6):1293 – 1304, 1989. ISSN 0004-6981. doi:http://dx.doi.org/10.1016/0004-6981(89)90153-4.

J. Williams, V. Gros, E. Atlas, K. Maciejczyk, A. Batsaikhan, H. F. Schöler, C. Forster, B. Quack, N. Yassaa, R. Sander, and R. Van Dingenen. Possible evidence for a connection between methyl iodide emissions and Saharan dust. *Journal of Geophysical Research: Atmospheres*, 112(D7):n/a–n/a, 2007. ISSN 2156-2202. doi:10.1029/2005JD006702. URL http://dx.doi.org/10.1029/2005JD006702. D07302.

M. Yang, R. Beale, P. Liss, M. Johnson, B. Blomquist, and P. Nightingale. Air-sea fluxes of oxygenated volatile organic compounds across the Atlantic Ocean. *Atmospheric Chemistry and Physics*, 14(14):7499–7517, 2014. doi:10.5194/acp-14-7499-2014. URL http://www.atmos-chem-phys.net/14/7499/2014/.

X. Yang, R. A. Cox, N. J. Warwick, J. A. Pyle, G. D. Carver, F. M. O'Connor, and N. H. Savage. Tropospheric bromine chemistry and its impacts on ozone: A model study. *Journal of Geophysical Research: Atmospheres*, 110(D23):n/a–n/a, 2005. ISSN 2156-2202. doi:10.1029/2005JD006244. URL http://dx.doi.org/10.1029/2005JD006244. D23311.

R. A. Zaveri, R. C. Easter, J. D. Fast, and L. K. Peters. Model for Simulating Aerosol Interactions and Chemistry (MOSAIC). *Journal of Geophysical Research: Atmospheres*, 113(D13):n/a–n/a, 2008. ISSN 2156-2202. doi:10.1029/2007JD008782. URL http://dx.doi.org/10.1029/2007JD008782. D13204.

F. Ziska, B. Quack, K. Abrahamsson, S. D. Archer, E. Atlas, T. Bell, J. H. Butler, L. J. Carpenter, C. E. Jones, N. R. P. Harris, H. Hepach, K. G. Heumann, C. Hughes, J. Kuss, K. Krüger, P. Liss, R. M. Moore, A. Orlikowska, S. Raimund, C. E. Reeves, W. Reifenhäuser, A. D. Robinson, C. Schall, T. Tanhua, S. Tegtmeier, S. Turner, L. Wang, D. Wallace, J. Williams, H. Yamamoto, S. Yvon-Lewis, and Y. Yokouchi. Global sea-to-air flux climatology for bromoform, dibromomethane and methyl iodide. *Atmospheric Chemistry and Physics*, 13(17):8915–8934, 2013. doi:10.5194/acp-13-8915-2013. URL http://www.atmos-chem-phys.net/13/8915/2013/.